Systematic study of 1,2,3-triazolyl sterols for the development of new drugs against parasitic Neglected Tropical Diseases.

Exequiel O. J. Porta,[a,#,†] María Sol Ballari,[a,#] Renzo Carlucci,[a,#] Shane Wilkinson,[b] Guoyi Ma,[c] Babu L. Tekwani,[c,] and Guillermo R. Labadie.[a,d,*]

[a] *Instituto de Química Rosario (IQUIR-CONICET), Facultad de Ciencias Bioquímicas y Farmacéuticas, Universidad Nacional de Rosario. Suipacha 531, S2002LRK, Rosario, ARGENTINA*

[b]*. Queen Mary, University of London, Mile End Road, London E1 4NS, UK.*

[c] *Department of Infectious Diseases, Division of Scientific Platforms, Southern Research, Birmingham, AL 35205, USA*

[d] *Departamento de Química Orgánica, Facultad de Ciencias Bioquímicas y Farmacéuticas, Universidad Nacional de Rosario, Suipacha 531, S2002LRK, Rosario, ARGENTINA.*

[#] *The authors have contributed equally.*

[†] *Present address: Department of Chemistry, Durham University, Durham, DH1 3LE, UK.*

* *Corresponding author*

E-mail: labadie@iquir-conicet.gov.ar

Phone number: +54-341-4370477 # 108

FAX number: +54-341-4370477 # 112

Abstract

A series of thirty 1,2,3-triazolylsterols, inspired by azasterols with proven antiparasitic activity, were prepared by a stereocontrolled synthesis. Ten of these compounds constitute chimeras/hybrids of 22,26-azasterol (AZA) and 1,2,3-triazolyl azasterols. The entire library was assayed against the kinetoplastid parasites *Leishmania donovani*, *Trypanosoma cruzi*, *and Trypanosoma brucei*, the causatives agents for visceral leishmaniasis, Chagas disease, and sleeping sickness, respectively. Most of the compounds were active at submicromolar/nanomolar concentrations with high selectivity index, when compared to their cytotoxicity against mammalian cells. Analysis of *in silico* physicochemical properties were conducted to rationalize the activities against the neglected tropical disease pathogens. The analogs with selective activity against *L. donovani* (**E4**, IC_{50} 0.78 μM), *T brucei* (**E1**, IC_{50} 0.12 μM) and *T. cruzi* (**B1**- IC_{50} 0.33 μM), and the analogs with broad-spectrum antiparasitic activities against the three kinetoplastid parasites (**B1** and **B3),** may be promising leads for further development as selective or broad-spectrum antiparasitic drugs.

Keywords: Antiparasitic, azasterols, Click chemistry, kinetoplastid diseases, NTDs.

1. Introduction

Neglected tropical diseases (NTDs) are a diverse group of twenty conditions that prevail in tropical and subtropical areas in more than 150 countries, affecting more than one billion people worldwide (>15% of the world's population) [1]. NTDs cost developing economies billions of dollars every year and are a significant source of morbidity and socioeconomic burden, particularly among the world's poorest countries [2]. Populations living in poverty, without adequate sanitation and in close contact with vectors, domestic animals, and livestock, are usually at higher risks for contracting these infections.

NTDs also pose a major challenge for global public health and impose a huge burden for both health and economy. NTDs, simultaneously, constitute a serious obstacle to achieving socioeconomic development and a good quality of life. In spite of this, these ailments have received little attention and have been delayed in public health priorities [3]. During the last decade, diverse alliances between public and private sectors have turned the attention of global and government health agencies to these diseases, highlighting the fight to treat, control, contain, and eradicate these conditions [4,5].

Trypanosomatids are responsible for several NTDs that cause significant morbidity and mortality in millions of people and animals worldwide [6]. *Leishmania* spp. are the causative agents of cutaneous, mucocutaneous, and visceral leishmaniasis, affecting 12 million people in 98 countries in several continents. *Leishmania* spp. has a two-part life cycle with the promastigote form residing in the sand fly vector and the intracellular amastigote form in the mammalian host. On the other hand, *Trypanosoma cruzi* is the etiologic agent of Chagas disease, an endemic disease in the Americas, affecting 8 million people. *T. cruzi* has a complex life cycle involving four main stages: epimastigotes and metacyclic trypomastigotes in the triatomine vector, and bloodstream trypomastigote and intracellular amastigote in the mammalian host. Finally, the *Trypanosoma brucei* group is responsible for human African trypanosomiasis (HAT), also known as sleeping sickness, which affects people in Sub-Saharan Africa and nagana, a disease that affects cattle. *T. brucei* has four well-studied stages: namely, procyclic trypomastigotes in the tsetse fly vector midgut, epimastigotes when leave the midgut, metacyclic trypomastigote in the tsetse fly salivary gland, and

bloodstream trypomastigotes in the mammalian host. All these parasites represent a significant public health challenge and require effective interventions for their control and management. The distinct life cycle stages of these parasites play a crucial role in the transmission, pathology, and diagnosis of these parasites, making them important targets for therapeutic and diagnostic interventions [7].

The drugs available for the prophylaxis and treatment of these diseases are scarce, inadequate in terms of efficiency, often toxic, and possess several undesirable side effects. In addition, vaccines against these diseases are not available on the market yet, and the current treatments are usually expensive and difficult to administrate. Additionally, every year the reports of clinical cases containing multidrug-resistant parasites to conventional drugs are increasing [8–10].

At this point, it is imperative to not only develop new and better forms of diagnosis, prophylaxis, but also to develop new affordable and safer chemotherapies [11]. To address the critical task of identifying New Chemical Entities (NCE) against parasitic NTDs, different strategies can be followed. The selection of adequate molecular targets should consider the essentiality, the druggability and the presence or absence of orthogonal proteins in the host [12].

Trypanosomatids have an essential requirement for specific endogenous C28 sterols [13]. These sterols are critical for sustaining the structural and functional integrity of the cellular membranes and the cell cycle. On the other hand, trypanosomatids cannot use cholesterol (a C27 sterol), present in abundance in their vertebrate hosts, to meet these requirements. This property makes the trypansomatids susceptible to ergosterol biosynthesis inhibitors (EBIs).

Ergosterol biosynthesis is considered a vital metabolic pathway in fungi and members of the *Trypanosomatidae* family. In these organisms, this pathway produces a special class of sterols, absent in mammalian host cells [14], that includes ergosterol and other C24-methylated sterols. Ergosterol is required for growth and viability and differs structurally from cholesterol. Cholesterol contains only a single double bond in ring B, is completely saturated in the side chain and does not contain a methyl group at C24 (**Figure 1A**). Those differences are associated to divergent biosynthetic pathways that provide interesting targets for drug development.

Ergosterol biosynthesis has some molecular targets that are excellent candidates to identify NCEs, for instance C14-Demethylase (target for action of triazole inhibitors) or C24-Sterolmethyltransferase (target for action of azasterols), among others [15].

C24-Sterolmethyltransferase (24-SMT or SMT), also known as ERG6, catalyses the insertion of a methyl group from AdoMet in the sterol C24 side chain in a key process for the biosynthesis of sterols in plants, fungi, and parasites [16]. Zymosterol is the main substrate of the enzyme that is converted to fecosterol (**Figure 1B**). Although zymosterol is the preferred substrate for 24-SMT, this enzyme is also capable of methylating other sterol intermediates in the ergosterol biosynthetic pathway. This enzyme has no counterpart or homologue in mammals. SMT would constitute the limiting step in many of the biosynthetic pathways of the organisms where it is present [17]. According to the TDR targets database, SMT/ERG6 is classified as highly druggable, so SMT is an ideal molecular target for discovery of new drugs against these parasitic NTDs [18]. Additionally, the critical role of the enzyme on the mitochondrial functional and virulence on *L. major* has been demonstrated [19].

Azasterols (**Figure 1A**) are potent inhibitors of ergosterol biosynthesis, whose effects have been studied against *T. cruzi*, *Leishmania* spp*.,* and *T. brucei* [20,21], as well as *Candida* spp. The antiparasitic and antifungal activity of those azasterols is linked to the inhibition of 24-SMT. The sterol side chain in azasterols contains nitrogen atoms, which mimics the postulated transition state for enzyme mechanism [22], interrupting the ergosterol biosynthesis.

We have previously reported a collection of triazolyl sterols (**Figure 1A**) with activity in the low micromolar range against *Leishmania donovani* [23], the causative agent for visceral leishmaniasis. This library was further expanded for exploring new functionalities in this series of compounds. A collection of thirty 1,2,3-triazolylsterols, inspired by azasterols, were prepared by a stereocontrolled synthesis and assayed against the kinetoplastid parasites *L. donovani*, *T. cruzi,* and *T. brucei*, the causatives agents for visceral leishmaniasis, Chagas disease, and sleeping sickness, respectively.

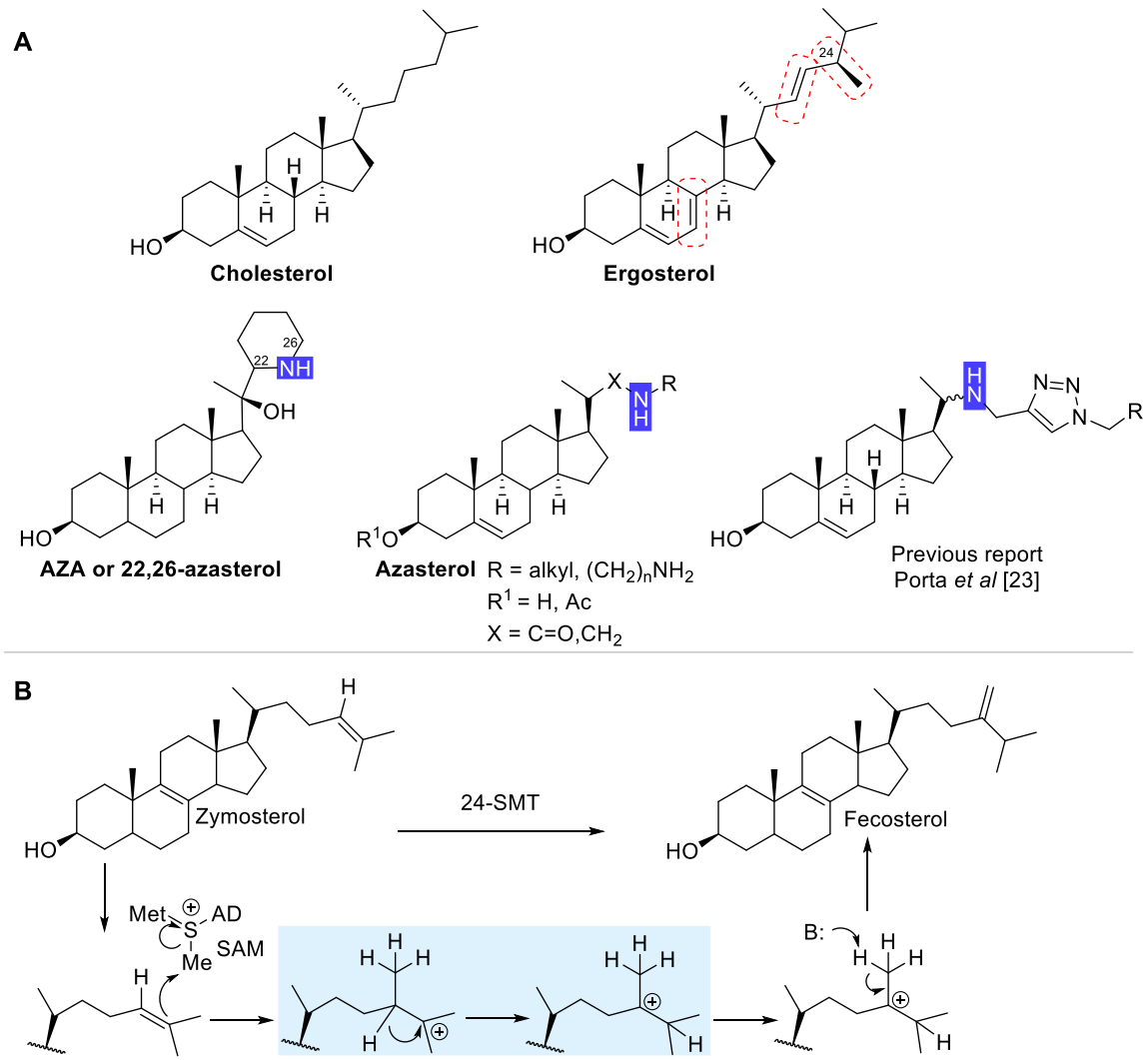

Figure 1. A) Structural differences between cholesterol and ergosterol (highlighted in red box); structures of AZA, azasterols, and triazolyl sterols previously reported by our group [23] which potentially target C24-Sterol methyl transferase. B) Proposed mechanism of the enzymatic reactions catalyzed by 24-SMT.

2. Results and discussion

2.1. Library design

Based on the models postulated by Nes [24,25] and Gilbert [26], we proposed specific structural modifications for preparation of our first-generation set of the compounds (Compounds **A1** to **B5**, **Table 1**), preserving essential and critical features of the series. First, the stereochemistry of the sterol ring, which is identical to ergosterol, was conserved (**Figure 2**). Second, the C3 hydroxy group that is essential for anchoring to the enzyme, was also preserved. Additionally, Gilbert and others [22,27] have concluded that azasteroids presenting C3 alcohol as acetate, in addition to a nitrogen

in the side chain, displayed a significant activity against *T. brucei rhodesiense*. These modifications increased the lipophilicity, facilitating the compounds to permeate the parasite membrane. These analogs are intracellularly hydrolyzed by esterases, to properly interact with the 24-SMT [22]. Accordingly, we decided to modify all the previously reported compounds, introducing an acetate on the C3-OH (**Figure 2-a**, compounds **C1** to **D5**, **Table 1**).

Another series of compounds were chimeras built by combination of the first-generation library (Compounds **A1** to **B5**, **Table 1**) with 22,26-azasterol (AZA, **Figure 1A**). AZA is one of the most studied azaterols, as a drug candidate for Chagas disease and leishmaniasis. It has been reported that AZA shows an interesting *in vitro* activity profile both in epimastigote and intracellular amastigote form of *T. cruzi*, as well as in *Leishmania* spp. AZA potentially acts by altering the composition of membrane sterols, causing cell disruption [22]. In addition, the preparation and antiparasitic activity of related compounds have been reported to show similar activity to AZA [21].

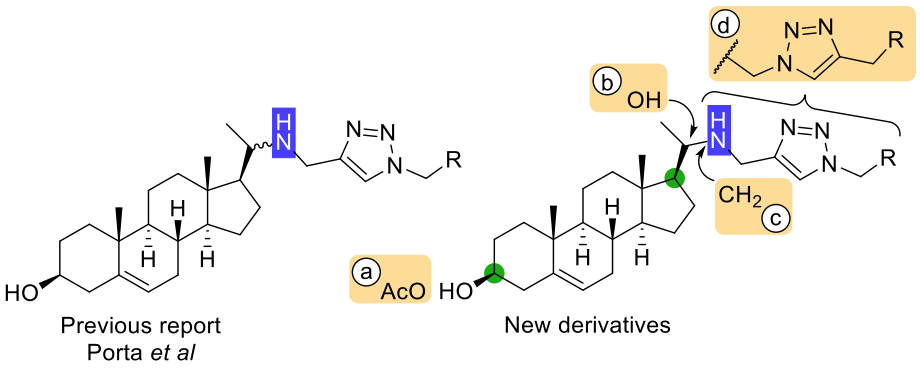

Figure 2. Design of the triazolyl sterol library.

The design of those chimeras was carried out conserving the amino alcohol scaffold in the sterol side chain, with the same configuration as ergosterol on C20 (**Figure 2-b**), spatially separated by two carbon atoms (**Figure 2-c**). A linear spatial arrangement for the amine was adopted instead of a cyclic one. The point of diversity was focused on the decoration of the 1,2,3-triazole motif, replaced by hydrophobic groups (Compounds **E1** to **E5**, **Table 1**).

At physiological pH, the secondary amino group on the side chain is protonated [22]. This could emulate the proposed carbocation intermediate for the enzyme reaction mechanism

(**Figure 1B**). To verify the essentiality of the secondary amino group, another set of analogs was prepared inverting the triazole substitution (**Figure 2-d**, compounds **F1** to **F5**, **Table 1**).

2.2. Synthesis

Starting from commercial pregnenolone, the corresponding acetate (**6**) was prepared with acetic anhydride in pyridine at room temperature, obtaining the expected product after 8 hours, with a 98% yield (**Scheme 1**). Then, the sterol was functionalized with a terminal alkyne and a secondary amine in the side chain, by reductive amination, with *N*-propargylamine, sodium triacetoxyborohydride, and in the presence of 4 Å molecular sieves, following our previously reported optimized procedure [23]. The two diastereoisomeric intermediates (Compounds **C** (*R*)-C20 and **D** (*S*)-C20) were efficiently separated by column chromatography, obtaining the products in a 1:1 ratio, with a 98% yield. The stereochemistry of the newly generated stereocenter at C20 was confirmed by comparison with the ^{1}H-NMR and ^{13}C-NMR signals with those prepared on the first-generation library [23]. On that opportunity, stereochemistry was unequivocally determined by the crystal structure of one of the isomers, confirming that compounds **B** and **D** have the same configuration as ergosterol.

Ten triazoles were generated by 1,3-dipolar cycloadditions catalyzed by Cu (I), using the same set of azides (namely, benzylazide, 2-azido-ethyl acetate, octyl azide, geranyl azide, and phenyl propyl azide) that were used to prepare the first-generation library. In this case, an average yield of 83% (Compounds **C1** to **D5**, **Table 1**) was obtained. Our group has previously reported that geranylazide exists in solution as a mixture of inseparable regioisomers [28,29], which after the cycloaddition stage allows to generate the *E* and *Z* isomers in a 3:2 ratio [30,31]. Although in some cases it is possible to separate the *E* and *Z* triazoles obtained from this azide mixture, in this case, due to the polarity of both diasteroisomers, all attempts to obtain pure isomers by chromatographic separation were unsuccessful.

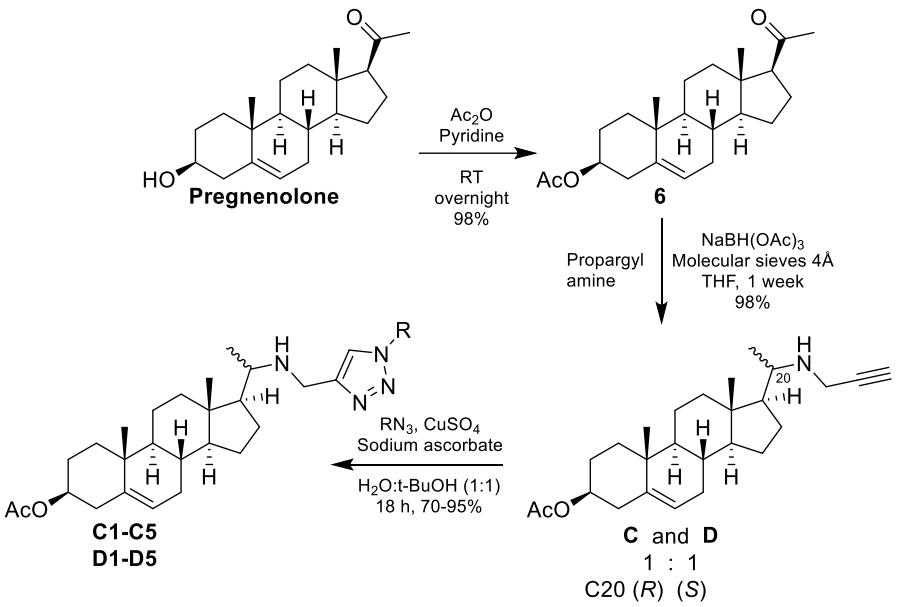

Scheme 1. Synthesis of libraries of **C** and **D** series.

For families **E** and **F**, we used a divergent synthetic strategy from a common precursor (**Scheme 2**). Here, starting from pregnenolone, the C3-alcohol was protected as a silyl ether, using tert-butyldimethylsilyl chloride (TBDMS-Cl) and imidazole, in DMF. The expected product (**7**) was obtained after 12h, with a 93% yield. Then, the next step involved the epoxidation of the pregnenolone through the Johnson-Corey-Chaykovsky reaction. The ilium was prepared using trimethylsulfoxonium iodide and sodium hydride in DMSO at 0 °C for 2 hours. Subsequently, the protected ketosterol was added and the reaction mixture was left for a further 20 hours [32]. Under these conditions a single diastereoisomer (**8**, 20*R*) was obtained with 91% yield. The selectivity of this reaction has been previously reported [33], and is primarily due to the high reactivity of dimethylsulfonium methylide. This sulphur ilium reacts faster by the less hindered face of the ketone. The epoxide configuration was confirmed by comparison of the ^{1}H NMR spectrum signals of the two oxirane protons and structures previously reported in the literature [34,35].

This epoxide **8** constitutes a valuable intermediate in our strategy, since it is possible to open it with a wide variety of nucleophilic or acid reagents, being a convenient diversity entry point.

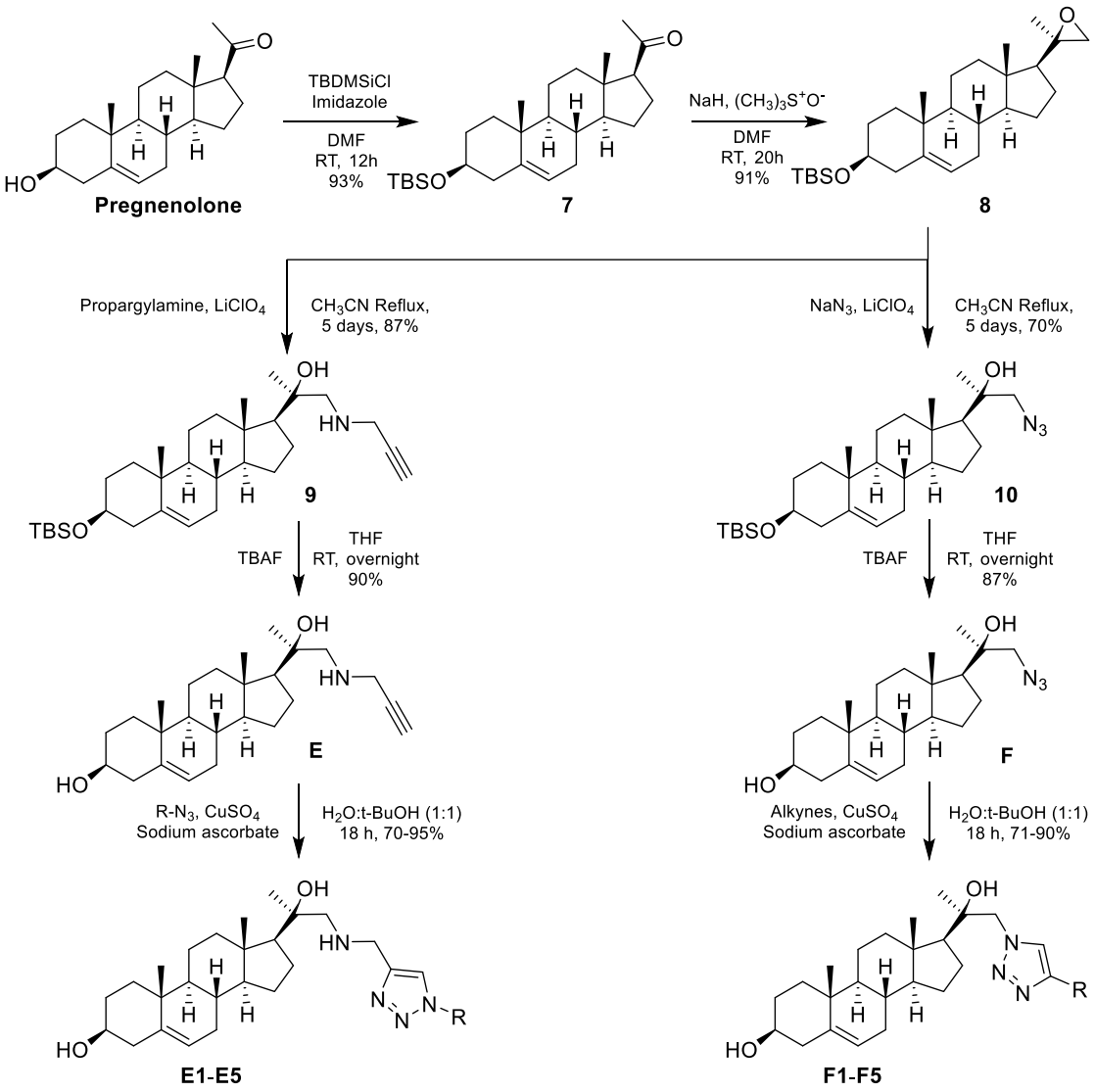

Scheme 2. Synthesis of steryl-1,2,3-triazoles series **E** and **F**.

The epoxide was separately opened with NaN_3, or with *N*-propargylamine, in the presence of $LiClO_4$ in acetonitrile at reflux for 5 days [36]. The reaction provided the expected amino alkynylsterol **9** and the azide **10** intermediates with 87% and 70% yield, respectively. Once those intermediaries were generated, the alcohols were deprotected before the cycloaddition reaction using tetrabutylammonium fluoride in THF for 12 hours, at room temperature, affording the alkynylsterol **E** and azidosterol **F** with 90% and 87% yield, respectively.

Then, the copper-catalyzed cycloaddition of the alkyne **E** with the same set of azides used before provided the hydroxyamino 1,2,3-triazolyl sterols **E1** - **E5** (**Table 1**), with an average yield of 81%. Similarly, the reactions of azide **F** with five terminal alkynes, stereoelectronically

similar to the set of azides used before, provided the expected triazoles, with an average yield of 83% after the cycloaddition step (**F1** to **F5**, **Table 1**).

Table 1. 1,2,3-triazolyl sterols synthesized in this work.

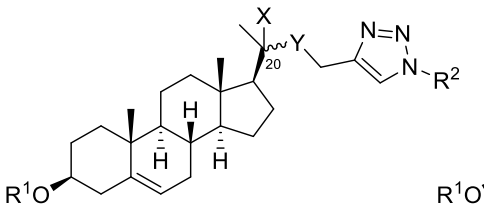

Series A-E

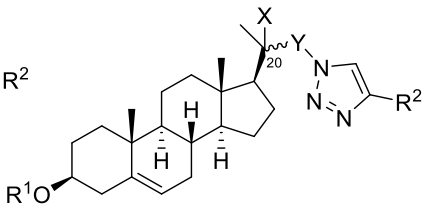

Series F

Series	Cmpd	R^1	X	Y	R^2	(C20)	Yield (%)
	A1	H	H	NH	Bn	*R*	89
	A2	H	H	NH	CH_2COOEt	*R*	78
A	**A3**	H	H	NH	Octyl	*R*	83
	A4	H	H	NH	Geranyl	*R*	90
	A5	H	H	NH	$Ph(CH_2)_3$	*R*	94
	B1	H	H	NH	Bn	*S*	76
	B2	H	H	NH	CH_2COOEt	*S*	78
B	**B3**	H	H	NH	Octyl	*S*	75
	B4	H	H	NH	Geranyl	*S*	94
	B5	H	H	NH	$Ph(CH_2)_3$	*S*	90
	C1	Ac	H	NH	Bn	*R*	90
	C2	Ac	H	NH	CH_2COOEt	*R*	86
C	**C3**	Ac	H	NH	Octyl	*R*	76
	C4	Ac	H	NH	Geranyl	*R*	80
	C5	Ac	H	NH	$Ph(CH_2)_3$	*R*	85
	D1	Ac	H	NH	Bn	*S*	83
	D2	Ac	H	NH	CH_2COOEt	*S*	70
D	**D3**	Ac	H	NH	Octyl	*S*	81
	D4	Ac	H	NH	Geranyl	*S*	88
	D5	Ac	H	NH	$Ph(CH_2)_3$	*S*	95
	E1	H	OH	CH_2NH	Bn	*R*	79
	E2	H	OH	CH_2NH	CH_2COOEt	*R*	90
E	**E3**	H	OH	CH_2NH	Octyl	*R*	85
	E4	H	OH	CH_2NH	Geranyl	*R*	81
	E5	H	OH	CH_2NH	$Ph(CH_2)_3$	*R*	71
	F1	H	OH	CH_2	Ph	*R*	69
	F2	H	OH	CH_2	COOMe	*R*	73
F	**F3**	H	OH	CH_2	Pentyl	*R*	86
	F4	H	OH	CH_2	CH_2CH_2OH	*R*	97
	F5	H	OH	CH_2	$Ph(CH_2)_3$	*R*	92

2.3. Biological activity

The *in vitro* antiparasitic activity of the entire collection of 30 compounds and its intermediates was assessed against *L. donovani*, *T. brucei,* and *T. cruzi* (**Table 2**). In detail, the activity as antileishmanial agents was carried out on *L. donovani* promastigotes, the main etiological agent of the visceral form of the disease. The IC_{50}s against *T. cruzi*, the protozoan

parasite that causes Chagas' disease in American continent, were determined on the epimastigote form. The action against bloodstream form *T. brucei*, that causes sleeping sickness disease or Human African Trypanosomiasis (HAT), was evaluated. In addition, the IC_{50} values of commercial drugs for each disease were determined, as a positive control, namely, pentamidine and amphotericin B for leishmaniasis, benznidazole and nifurtimox for Chagas disease, and melarsoprol for HAT. DMSO was used as a negative control. Finally, cytotoxicity was evaluated against African green monkey kidney epithelial cell line (VERO cells), a standard model.

The activity on *L. donovani* promastigotes of 10 analogues and 2 intermediates (compounds **A**, **A1** - **A5**, **B**, **B1** - **B5**) has been previously reported by our group [23]. The new analogues and intermediates were assayed against *L. donovani*. To our satisfaction, most of the compounds were active against this parasite (**Table 2**). An 80% of the whole collection exhibited an IC_{50} below 10 µM, with 56% of the library being more potent than pentamidine, one of the reference drugs against leishmaniasis. Compound **E4** (IC_{50} = 780 nM) was the most potent of the collection, with an activity in the same order as Amphotericin B (IC_{50} = 350 nM) and more than 8 times more potent than pentamidine (IC_{50} = 6.17 µM).

Looking for active compounds against the etiological agent of African trypanosomiasis, the library was tested *in vitro* against *T. brucei* (**Table 2**). In this case, more than 86% of the compounds of our collection were active against this parasite at concentrations lower than 10 µM. Even half of this library was active against *T. brucei* at submicromolar concentrations. Although none of the compounds have activities on the order of Melarsoprol (10 nM), the activities against *T. brucei* are very promising, especially considering that this commercial drug is an arsenic derivative that not only has numerous side effects, but also very high mortality rates. The best compound in the entire library is the chimeric **E1** (IC_{50} = 120 nM). However, there are other four compounds with activities between 180 to 200 nM (compounds **C5**, **D1**, **D5**, and **F3**). All of them (except for **F3**) contain aromatic substituents on the 1,2,3-triazole.

Table 2. Antiparasitic activities and mammalian cell cytotoxicity of new 1,2,3-triazolylsterols.[a]

Comp	***L. donovani*** **promastigotes**		***T. brucei*** **bloodstream form**		***T. cruzi*** **epimastigotes**		***Cytotoxicity*** **VERO cells**
	IC_{50} µM[b]	**S.I.**	**IC_{50} µM[c]**	**S.I.**	**IC_{50} µM[c]**	**S.I.**	**IC_{50} µM**
A	> 10	ND	> 10	ND	2.03	> 6.57	> 13.3
A1	6.14	> 1.67	1.77 ± 0.06	> 5.78	2.47 ± 0.21	> 4.14	> 10.2
A2	6.60	> 1.56	6.50 ± 0.10	> 1.59	> 10	ND	> 10.3
A3	2.55	> 3.85	1.50 ± 0.22	> 6.53	> 10	ND	> 9.79
A4	1.14	> 8.20	0.66 ± 0.02	> 14.2	> 10	ND	> 9.35
A5	1.94	> 5.00	1.82 ± 0.08	> 5.18	6.48 ± 0.03	> 1.45	> 9.42
B	4.50	> 2.98	> 10	ND	1.27	> 10.5	> 13.3
B1	1.33	> 7.69	0.68 ± 0.01	> 15.0	0.33 ± 0.04	> 31.0	> 10.2
B2	6.40	> 1.61	> 10	ND	> 10	ND	> 10.3
B3	1.47	> 6.67	0.55 ± 0.02	> 17.8	1.95 ± 0.09	> 5.02	> 9.79
B4	1.68	> 5.56	0.64 ± 0.01	> 14.6	3.17 ± 0.21	> 2.95	> 9.35
B5	1.35	> 7.14	1.43 ± 0.15	> 6.77	2.22 ± 0.03	> 4.36	> 9.68
C	> 10	ND	5.03 ± 0.31	> 2.30	> 10	ND	> 11.9
C1	> 10	ND	1.15 ± 0.10	> 6.22	> 10	ND	> 7.16
C2	> 10	ND	6.50 ± 0.10	> 1.46	> 10	ND	> 9.49
C3	> 10	ND	1.98 ± 0.03	> 4.57	> 10	ND	> 9.04
C4	10.3	> 0.84	1.25 ± 0.18	> 6.93	> 10	ND	> 8.67
C5	> 10	ND	0.20 ± 0.00	> 44.7	4.50 ± 0.09	> 1.99	> 8.95
D	> 10	ND	1.80 ± 0.10	> 6.44	8.88 ± 0.08	> 1.31	> 11.9
D1	2.54	> 3.70	0.20 ± 0.00	> 47.1	2.55 ± 0.05	> 3.69	> 9.42
D2	4.90	> 1.94	0.66 ± 0.01	> 14.4	7.80 ± 0.17	> 1.22	> 9.49
D3	7.87	> 1.15	0.62 ± 0.01	> 14.6	> 10	ND	> 9.04
D4	4.83	> 1.79	0.63 ± 0.03	> 13.8	> 10	ND	> 8.67
D5	2.99	> 2.99	0.20 ± 0.01	> 44.7	6.30 ± 0.26	> 1.42	> 8.95
E	> 10	ND	1.77 ± 0.12	> 6.95	> 10	ND	> 12.3
E1	1.95	> 4.95	0.12 ± 0.03	> 80.3	8.28 ± 0.10	> 1.16	> 9.64
E2	> 10	ND	> 10	ND	> 10	ND	> 9.71
E3	1.46	> 6.33	0.63 ± 0.03	> 14.7	8.13 ± 0.08	> 1.14	> 9.24
E4	0.78	> 11.4	0.65 ± 0.01	> 13.6	9.00 ± 0.05	> 0.98	> 8.85
E5	1.04	> 8.77	> 10	ND	> 10	ND	> 9.14
F	> 10	ND	> 10	ND	> 10	ND	> 12.0
F1	> 10	ND	> 10	ND	> 10	ND	> 10.5
F2	> 10	ND	8.28 ± 0.26	> 1.28	> 10	ND	> 10.6
F3	> 10	ND	0.18 ± 0.01	> 59.8	6.33 ± 0.31	> 1.68	> 10.6
F4	> 10	ND	1.78 ± 0.08	> 6.33	> 10	ND	> 11.3
F5	> 10	ND	2.27 ± 0.06	> 4.25	> 10	ND	> 9.66
Pent	6.17	7.6					47 [37]
AmpB	0.35	20					7.03 [38]
Mel			0.20	62.5			12.5 [39][d]
Ben					7.4	1.9	14 [37]
Nif			1.70 ± 0.10	18.8	2.10 ± 0.10	15.2	32 [37]

[a] SI (selectivity index) = $IC_{50\ Vero}$ / $IC_{50\ parasite}$. Pent: Pentamidine, AmpB: Amphotericin B, Mel: Melarsoprol, Ben: Benznidazole, and Nif: Nifurtimox. ND: not determined. [b] IC_{50}s are expressed as the average of two independent measurements. [c] IC_{50}s are expressed as average ± SD of three independent measurements. [d] Reported cytotoxicity on MRC-5 cells [39].

Finally, all the final products (**A1** – **F5**) and their synthetic intermediates (**A** – **F**) were tested *in vitro* against *T. cruzi* (**Table 2**). In this case, 47% of compounds showed an activity below 10 µM. Surprisingly, more than 30% of the tested analogues had better activities than the two commercial control drugs (Nifurtimox and Benznidazole). The most promising member is **B1** (IC_{50} = 330 nM), a compound 24 and 22 times more active than Nifurtimox (IC_{50} =7.7 µM) and Benznidazole (IC_{50} =7.4 µM), respectively. Also, **B1** is the only active member at submicromolar concentration. It is noteworthy that the intermediates **A** (IC_{50} = 2.03 µM) and **B** (IC_{50} = 1.27 µM) also presented great activity profiles against this parasite. Both intermediates with terminal alkynes can become excellent chemical probes to study both the mechanisms of action of these compounds on parasites and to carry out activity-based protein profiling (ABPP) studies.

It has been postulated that azasterols can mimic the carbocation mechanistic intermediate, and Gilbert's group has explored that hypothesis preparing compounds containing nitrogen on the sterol lateral chain. These compounds showed an enzyme inhibition profile well correlated with their antiparasitic activity, validating sterol methyltransferase as a druggable target [22], being AZA (**Figure 1A**) their lead compound. We were able to find compounds more potent than AZA against each parasite. In *T. brucei*, 76% of our library showed a better activity profile than AZA (IC_{50} = 3.3 µM [21]). Our top 5 compounds (**E1**, **F3**, **D1**, **D5**, **C5**) were between 16 and 27 times more potent, compared to AZA. In *T. cruzi*, only **B1** (IC_{50} = 0.33 µM) had a better activity than AZA (IC_{50} = 0.94 µM [22]), the former being 3 times more potent than the latter. For *L. donovani*, it was remarkable that all the compounds from **E** family (with exception of **E2**) resulted in a 10-fold increment in activity, compared to AZA, which caused growth inhibition of *L. donovani* promastigotes with IC_{50} of 12 µM [22]. This highlights the success in the construction of the chimera family between our reported library and AZA. Therefore, these chimeric compounds may be excellent starting points for the optimization and development of new antileishmanial leads.

2.3.1. Cytotoxicity

Our library was tested for their effect on Vero cells to a maximum concentration of 4.75 µg/mL (between 8 to 11 µM). This cell line is an excellent model for test cytotoxicity *in vitro* because it is an

aneuploid and a continuous cell lineage. None of the compounds showed cytotoxicity at levels lower than those tested. This allows several compounds to have excellent selectivity index values towards parasites (**Table 2**).

For *L. donovani*, the most active compound **E4** has an IC_{50Vero} > 8.85 µM and an $IC_{50L.donovani}$ = 0.78 µM, hence its SI is > 11, moderately better than pentamidine (SI = 7.6). For *T. brucei*, there were several compounds with submicromolar activities, with a consequent enhanced selectivity. That is the case for analogues **E1** (IC_{50Vero} > 9.64 µM, $IC_{50T.brucei}$ = 120 nM, SI > 80), **F3** (IC_{50Vero} > 10.64 µM, $IC_{50T.brucei}$ = 180 nM, SI > 60), **D1** (IC_{50Vero} > 9.42 µM, $IC_{50T.brucei}$ = 200 nM, SI > 47), **D5** (IC_{50Vero} > 8.95 µM, $IC_{50T.brucei}$ = 200 nM, SI > 45) and **C5** (IC_{50Vero} > 8.95 µM, $IC_{50T.brucei}$ = 200 nM, SI > 45). For *T. cruzi*, **B1** presented an IC_{50Vero} > 10.23 µM and an $IC_{50T.cruzi}$ = 0.33 µM, which translated in SI > 31. This SI resulted in a 7 and 16-fold increment respect to nifurtimox and benznidazole's SIs, respectively. Therefore, those are promising candidates that can move forward to validation on the intracellular stages of *T. cruzi* and *L. donovani* (amastigotes). Those candidates with IC_{50} < 10 µM in amastigotes with SI > 10 will be moved forward to *in vivo* studies [40,41].

2.4. Structure Activity Relationship (SAR)

An activity heatmap that represents the results of the antiparasitic activities against *L. donovani*, *T. brucei*, and *T. cruzi* was prepared (**Figure 3**). The activity of each analog is represented by a color code, with dark green indicating high activity, and black low or no activity. Five modification centers were defined to understand how specific structural features influence their antiparasitic activity. These centers are the stereochemistry of C20; C3-OH, free hydroxy or acetylated (R^1); C20 substitution (X=OH or H); C20 bound to NH, CH_2NH, or $N_{triazole}$ (Y); and the nature of the triazole substituent (R^2). These modifications are presented on **Figure 4**.

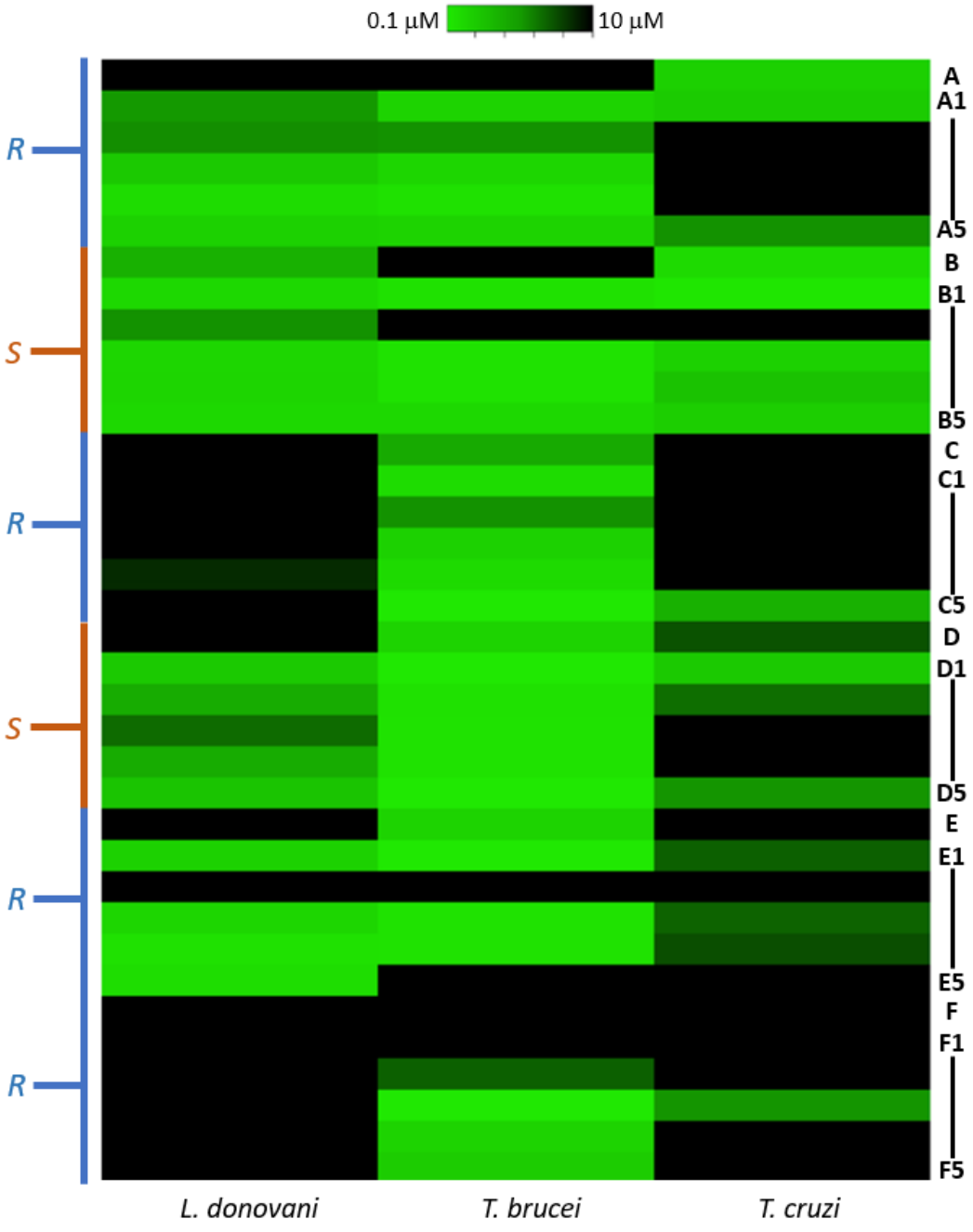

Figure 3. Anti-kinetoplastid activity heat map.

The C20 stereochemistry is relevant for the activity against all three parasites. Compounds with stereochemistry analogous to zymosterol (families **B** and **D**) are more active than their *(R)*-C20 analogues (families **A** and **C**). For example, in *L. donovani*, the average IC_{50} of series **B** ((*S*)-C20) was 2.45 µM, while series **A** ((*R*)-C20) had an average IC_{50} of 3.67 µM. The differences between the acetylated analogs **C** ((*R*)-C20) and **D** ((*S*)-C20) were more prominent. Series **D** had 5 active compounds with and average IC_{50} of 4.63 µM, while series **C** had only one borderline active analog (IC_{50} = 10.3 µM). A similar trend was observed for *T. brucei* and *T. cruzi*.

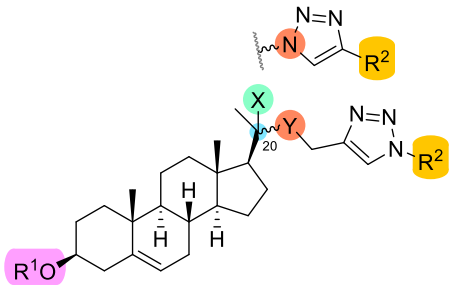

Figure 4. Fragments modified for SAR studies.

The IC_{50} comparison between families **A** and **C** or **B** and **D** showed that the presence of an acetyl group on the C3 (R^1) decreased the activity in *L. donovani* and *T. cruzi*, but it had the opposite effect on *T. brucei*, where the acetyl analogs were more active. For example, for *L. donovani*, the C3-OAc families **C** (1 active compound, IC_{50} = 10.3 µM) and **D** (average IC_{50} = 4.63 µM, 5 active compounds) led to a decrease in their potencies between two and three times on average, compared to the C3-OH families **A** (average IC_{50} = 3.67 µM, 5 active compounds) and **B** (average IC_{50} = 2.45 µM, 5 active compounds), respectively. A similar trend was observed for *T. cruzi*, where differences given by acetylation of C3 alcohol were more evident in the (*S*)-C20 series (families **B** and **D**). As was previously stated, the presence of a C3-OAc had an opposite effect for *T. brucei*, where the activity was improved, compared to the free alcohol analogs. In this case, families **A** and **B** (free C3-OH) presented average IC_{50}s of 2.45 µM and 0.82 µM, while acetyl families **C** and **D** presented improved average IC_{50}s of 1.14 µM and 0.46 µM, respectively. These results were expected and are consistent with those reported by Gilbert's group and others [22,27], where the acetates presented improved potency. Those results were interesting, since a small modification on the molecule, such as C3-OH acylation, can modulate the activity of the compounds towards the African or American variant of trypanosomiasis.

From the comparison of the activities of the **E** analogues with families **A** to **D**, it turned evident that the hydroxy group at C20 was relevant for the antiparasitic activity. The family **E** resulted the most active in average against *L. donovani* (1.31 µM, 4 active compounds). The positive effect coming from the alcohol at C20 for the chimeric compounds **E** was clear when the average potency was compared to the second most active family **B** (2.45 µM, 5 active compounds). Compound **E1** was the most active against *T. brucei*. Nevertheless, the activity of family **E** (average IC_{50} = 0.47 µM, 3

active compounds) was comparable to family **D** (average IC_{50} = 0.46 µM, 5 active compounds). This leads us to propose that compounds with hydroxy group C20 and an acetate at C3 would improve the anti-*T. brucei* activity. On the contrary, a hydroxy group at C20 was detrimental for the activity on *T. cruzi*, being the average IC_{50} of family **E** (8.47 µM) the weakest of the whole library, compared to families **A** (4.47 µM), **B** (1.92 µM), **C** (4.50 µM) and **D** (5.55 µM).

The presence of a basic, aliphatic, free amino group at Y is an important moiety for the antiparasitic activity of the compounds. This is suggested by the fact that family **F**, which replaced the secondary amine with an N-triazole, was less active than the other families in the series. For example, none of the compounds of the **F** family were active against *L. donovani* at 10 µM. Remarkably, **F3** was one of the most active analogs against *T. brucei*. However, average IC_{50} for the **F** family (3.13 µM) was not better than for the rest of the series (0.46 to 2.45 µM), and in consequence we consider **F3** as an exception to the general tendencies. For *T. cruzi*, only **F3** was active in this family.

Throughout all the compounds tested, it was evident that the ethyl acetate substituent at R^2 caused a decrease in activity for all parasites. This could be due to its lower lipophilicity and poor mimicking of the native sterol lipophilic side chain. For *L. donovani*, the best R^2 are phenylpropyl (average IC_{50} = 1.83 µM) and geranyl (average IC_{50} = 2.11 µM). For *T. brucei*, every lipophilic R^2 resulted in average IC_{50} in the single-micromolar range, being benzyl the best group (average IC_{50}: benzyl = 0.78 µM, octyl = 0.91 µM, geranyl = 0.94 µM, phenylpropyl = 1.18 µM). In *T. cruzi*, aromatic substituents resulted to be the preferred ones, with average IC_{50} of 3.41 µM for benzyl and 4.88 µM for phenylpropyl-substituted sterols.

2.5. *In silico* analysis of physicochemical parameters

The design of robust structures with physicochemical parameters that allow the crossing of various biological membranes is essential in drug development. This is particularly important for diseases like African trypanosomiasis where the blood-brain barrier must be crossed. Additionally, compounds that can be administered orally are desirable. Therefore, controlling physicochemical parameters during the drug design and optimization is crucial to identify the scaffold with good drug properties. Addressing pharmacokinetic properties in the early stages of drug development reduces the chances of failure in clinical trials and helps to reduce the time during the optimization process.

In silico physicochemical profile of the compounds prepared were conducted to predict their absorption, distribution, metabolism, and excretion properties (ADME), Lipinski's rule of five, the potential risks of toxicity, and to rationalize the biological activities found based on the structural modifications made.

The physicochemical parameters relevant for drug-target interaction, oral bioavailability and ADME-Tox, were calculated using Osiris DataWarrior [42], ChemAxon [43], SwissADME [44] and pkCSM [45] online platforms. Among the calculated properties, we included size (molecular weight, total surface area), polar interactions (polar surface area, number of H-bond donors and acceptors), lipophilicity (logP, logD), water solubility (logS), pharmacokinetics, toxicity, and druglikeness. The most relevant physicochemical parameters for the library are represented in histograms on **Figure 5** (complete data sets are presented in the Supporting Information), where a proper distribution of physicochemical properties was observed, with maximum count values at LogD = 5 – 6, cLogS = -6 – (-5.5), 2 H-bond donors, 6 H-bond acceptors, MW = 520 – 540 Da, total surface area = 400 – 420 $Å^2$, and polar surface area = 60 – 70 $Å^2$.

The predicted ADME-Tox properties suggested that all analogs are potential as lead compounds. The SwissADME analysis showed that the compounds did not present PAINS alerts. Although most of compounds violated at least one of Lipinski and Ghose rules, mostly due to high MW, they presented better Veber, Egan and Muegge parameters, achieving proper druglike parameters. According to pkCSM prediction, all active compounds presented good ADME-Tox properties. The library presented good absorption parameters, with a moderate Caco-2 permeability, high GI absorption, and good skin permeability. The volumes of distribution (VDss) rested moderate to high, and it is most likely that the compounds remain bound to serum proteins, as we could expect from their low solubility parameters, which could make the distribution process more difficult. The results also predicted the binding to CYP3A4, the main enzyme responsible for drug metabolism. Hence, the implications on the metabolism of these drugs should be further studied.

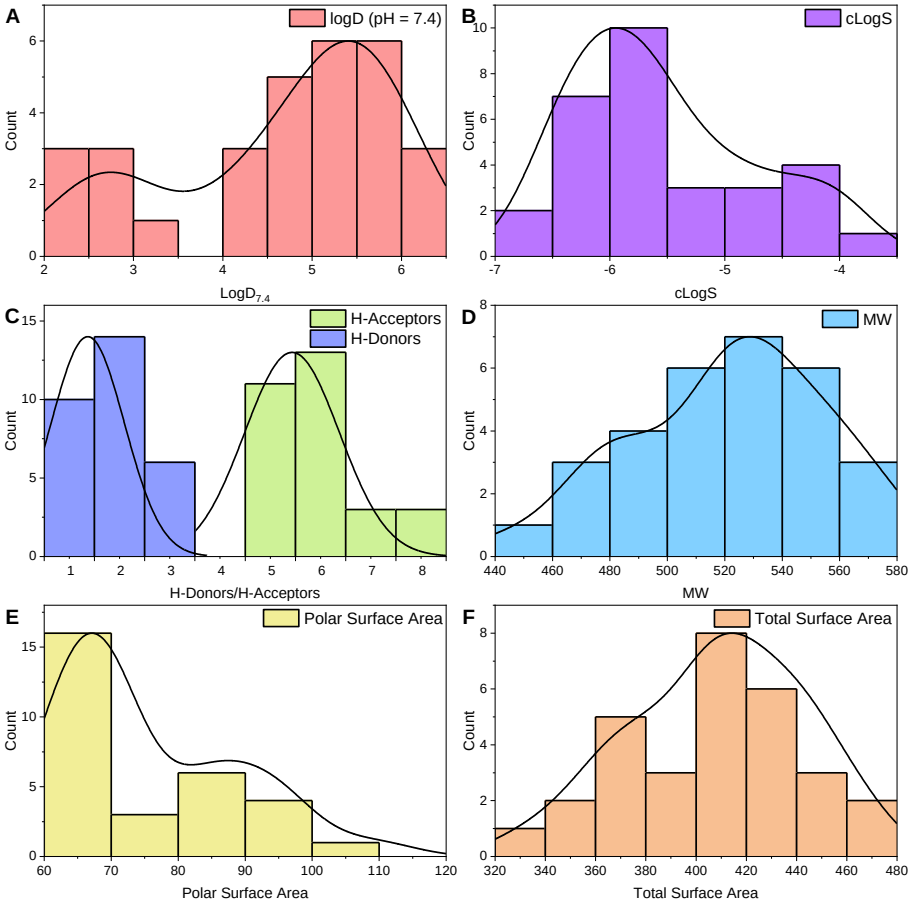

Figure 5. Physicochemical properties distribution for triazolyl sterols analogs. Distributions were fitted to Kernel Smooth function. A) LogD (pH = 7.4); B) cLogS; C) Hydrogen bond donors and acceptors; D) MW; E) Polar Surface Area; F) Total Surface Area.

Good clearance parameters were predicted for excretion, and the compounds did not present signs of being mutagenic, irritant, teratogenic, or toxic to sexual reproduction. All compounds presented hepatotoxicity alerts, which could be related to the CYP3A4 inhibition, and more studies should be made to address this issue.

To rationalize the lipophilicity requirements for the activity, a $logD_{7.4}$ vs IC_{50} for each parasite was plotted (**Figure 6**). Since our compounds have ionizable groups that are charged at physiological pH, logD (pH = 7.4) [46] resulted a better lipophilicity descriptor than cLogP, and the former was used in the analysis. Although there is no clear correlation between logD and IC_{50}, due to the high structural similarity between the analogs, we could determine logD zones where most active analogs are concentrated. For *L. donovani*, the most active compounds have logD between 4 and 5.6. *T.*

brucei seems to require compounds with logD greater than 4, and the requirements for *T. cruzi* are less clear since the collection resulted to be less active against this parasite. In this case, we found a small island of activity at logD between 4 and 5.5.

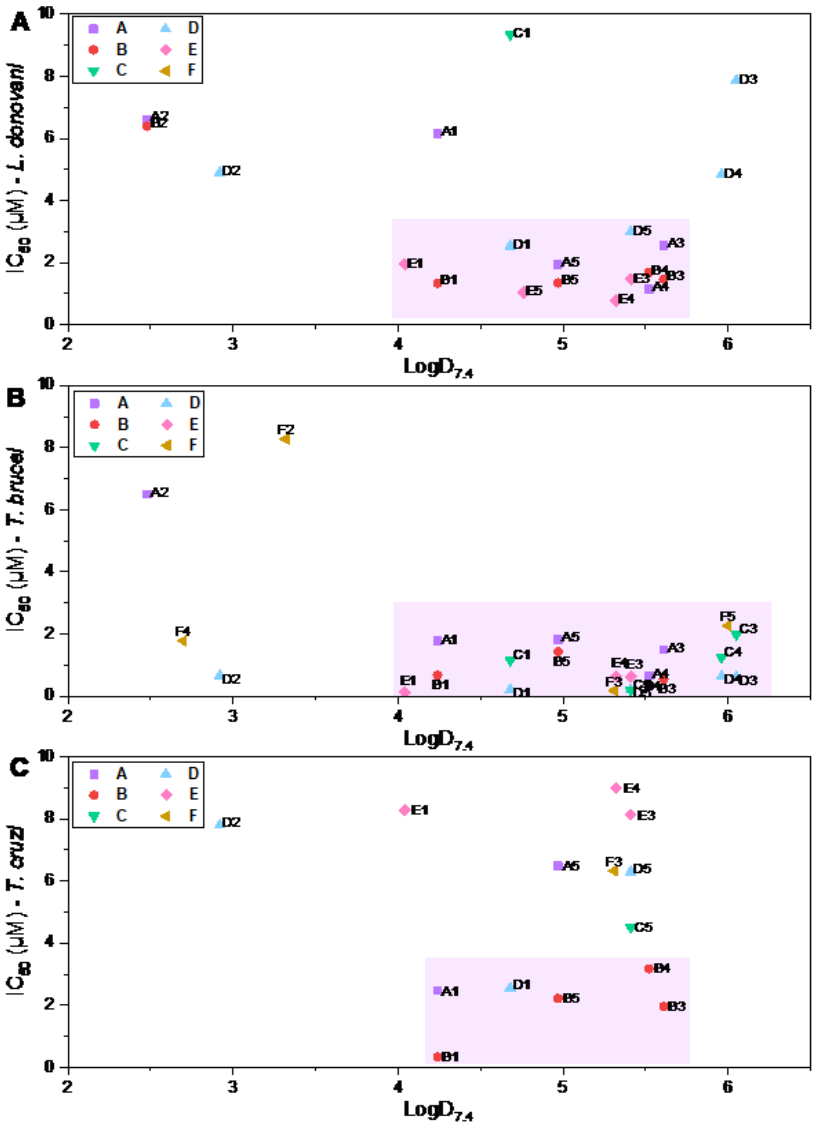

Figure 6. Correlation between antiparasitic activity and $logD_{7.4}$. A) *L. donovani*; B) *T. brucei*; C) *T. cruzi*.

In *T. brucei*, to be curative in the more serious cerebral phase of HAT the capability of a drug to permeate the CNS must be considered. Although the BBB permeability prediction by pkCSM and SwissADME indicate that the compounds would not be capable to permeate the brain-blood barrier, there is still a good chance that the compounds could permeate the CNS through other mechanisms (**Figure 7**). One critical parameter to determine if a compound could be able to penetrate the CNS

is the polar surface area (PSA), which usually does not exceed the 70 Å^2 for most of CNS penetrant drugs [47]. Generally, PSA values negatively correlate with passive CNS permeability, hence low PSA could translate in higher drug concentration in brain. It can be appreciated in **Figure 7** that many of the active compounds have proper CNS permeability (calculated as logPS: blood-brain permeability-surface area product), which correlates with their low PSA. It can be observed that the compounds included in the shadowed box in **Figure 7** mainly belong to the families **A**, **B**, **C** and **D**. These compounds will constitute excellent candidates to apply further structural optimization and improve brain penetration.

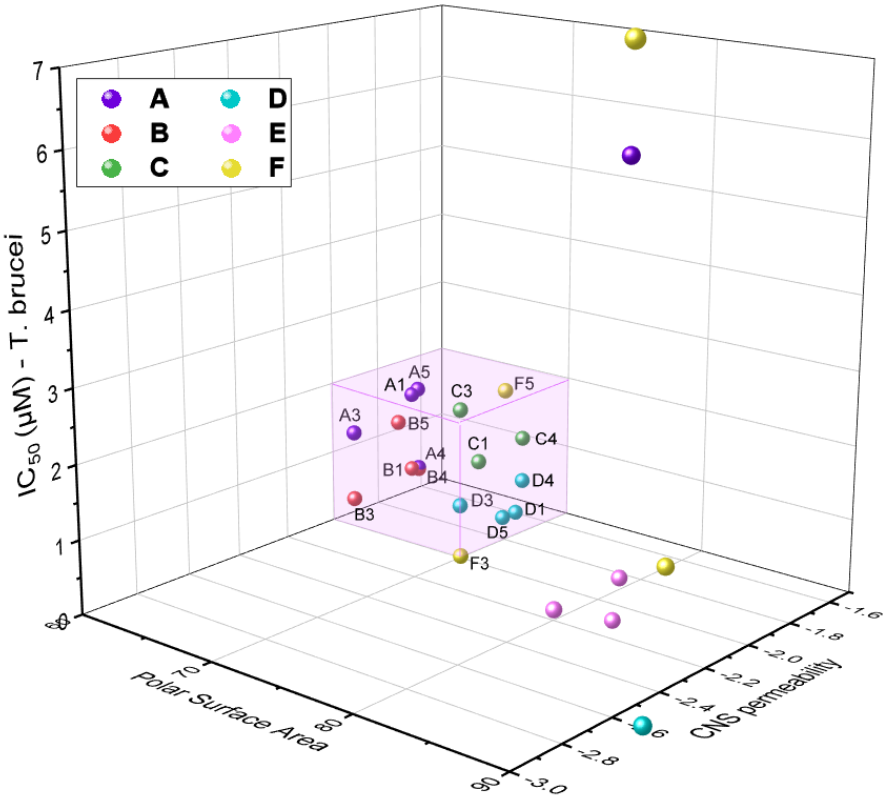

Figure 7. Correlation between anti-*T. brucei* activity, CNS permeability (logPS) and polar surface area. The shadowed box indicates the zone where the probability to permeate CNS is higher.

3. Conclusions

A library of 30 triazolyl sterols was successfully synthesized and characterized, with an average yield of 82% in the Cu(I) catalyzed cycloaddition. The synthesis of these triazolyl sterols were divided into 6 families. The first four (**A**, **B**, **C** and **D**) were prepared to emulate the carbocation intermediate of the enzyme 24-SMT. Families **C** and **D** have acetates, following the rational proposed by Nes

(improvement of permeability through the membrane and subsequent hydrolysis and action on target/s). Families **E** and **F** constitute a chimera/hybrid approximation between 22,26-Azasterol (AZA) and our first-generation library.

The selection of the best drug candidate as antiparasitic should combine low IC_{50} values with good physicochemical parameters, low cytotoxicity (high SI) and good CNS penetration (for *T. brucei*). **Figure 8** shows the structure – activity relationship found for our library against each of the tested parasites. Fortunately, none of the compounds showed cytotoxic activity against VERO cells at concentrations up to 10 µM.

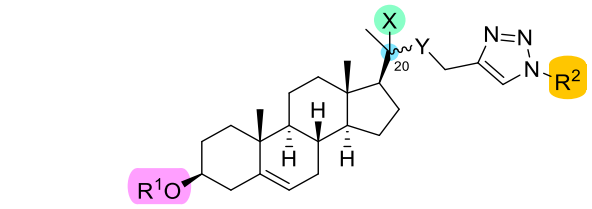

	L. donovani	*T. brucei*	*T. cruzi*
C_{20}	(*S*) > (*R*)	(*S*) > (*R*)	(*S*) > (*R*)
R^1	H > Ac	Ac > H	H > Ac
X	OH > H	OH > H	H > OH
R^2	$(CH_2)_3Ph$, geranyl	Bn, octyl, geranyl, $(CH_2)_3Ph$,	Bn, $(CH_2)_3Ph$
logD	4 - 5.6	> 4	4 - 5.5
Best for brain permeation		A, B, C, D	

Figure 8. Structure – activity relationship of our library as antiparasitic agents.

The compounds showed an excellent activity against *L. donovani*, with the most active compounds being 8 and 6 times more active than pentamidine, respectively (compound **E4**, IC_{50} = 780 nM, SI > 11.36; and, compound **E5**, IC_{50} = 1.04 µM, SI > 8.77). Both present good physicochemical and ADME-Tox properties and represent excellent candidates to move towards the next stage in the search for new antileishmanial agents. In this case, the chimera molecules constituted the best scaffold.

Chimeric **E1** (IC_{50} = 120 nM, SI > 80.32) was the most active candidate against *T. brucei*. Nonetheless, its higher polarity could be a downwards for a good CNS penetration and could not be used for treatment of cerebral phase of HAT. Compounds **C5**, **D1** and **D5**, all presenting an IC_{50} =

200 nM, with less polar groups, have the best properties for potential brain penetration and are excellent candidates for further structural optimization.

The most promising member against *T. cruzi* is **B1** (IC_{50} = 330 nM, SI > 31), a structure 24 times more active than Nifurtimox and 22 times more active than Benznidazole. In this case, this compound combines the best activity with excellent physicochemical properties, constituting a spearhead in the search for new anti-chagasic compounds. The activity and selectivity of **B1** against *L. donovani* (IC_{50} = 1.33 µM SI > 7.69) and *T. brucei* (IC_{50} = 0.68 µM SI > 15.0) make this analog the best candidate to develop a broad-spectrum anti-kinetoplastid drug.

The loss of activity of **F** family compounds allows us to successfully conclude the need to position a basic group on the side chain. This is in complete line with the hypothesis of the emulation of the carbocation intermediate.

Finally, based on the structural similarities between Gilbert's compounds and ours, it is possible that 1,2,3-triazolyl sterols can also interfere with the activity of sterol methyltransferase, and we plan on testing this hypothesis as we continue our work with 1,2,3-triazolylsterols.

4. Materials and Methods

4.1. General Information

^{1}H and ^{13}C NMR spectra were acquired on a Bruker Avance II 300 MHz (75.13 MHz) using $CDCl_3$ as solvent. Chemical shifts (δ) were reported in ppm downfield from tetramethylsilane (TMS) at 0 ppm as internal standard and coupling constants (*J*) are in hertz (Hz). Chemical shifts for carbon nuclear magnetic resonance (^{13}C NMR) spectra are reported in parts per million relatives to the center line of the $CDCl_3$ triplet at 76.9 ppm. The following abbreviations are used to indicate NMR signal multiplicities: s = singlet, d = doublet, t = triplet, q = quartet, m = multiplet, p = pentet, br = broad signal. High-resolution mass spectra (HRMS) were recorded on a Bruker MicroTOF II with lock spray source. IR spectra were obtained using an FTIR Shimadzu spectrometer and only partial spectral data are listed. Optical rotations were determined using a digital polarimeter Jasco DIP-100, the sodium D line (589 nm) as excitation wavelength. Cells were 100 mm long, and measurements were acquired at room temperature in the solvent and concentration indicated. Chemical reagents were purchased from commercial suppliers and used without further

purification, unless otherwise noted. Solvents were analytical grade or were purified by standard procedures prior to use. Yields were calculated for material judged homogeneous by thin layer chromatography (TLC) and nuclear magnetic resonance (^{1}H-NMR). All reactions were monitored by thin layer chromatography performed on silica gel 60 F_{254} pre-coated aluminum sheets, visualized by a 254 nm UV lamp, and stained with an ethanolic solution of 4-anisaldehyde. Column flash chromatography was performed using silica gel 60 (230–400 mesh).

4.2. Synthesis

4.2.1. Synthesis of pregnenolone acetate (6)

Pregnenolone (2.00 g, 6.33 mmol) was dissolved in pyridine (30 mL) at 0 °C. Then, acetic anhydride (30 mL) was added dropwise. The mixture stirred overnight at room temperature. Water (100 mL) was added, and the solution was extracted with AcOEt (3 x 50 mL). Combined organic phases were sequentially washes with 10% HCl (1 x 30 mL), 10% $NaHCO_3$ (1 x 30 mL), water (2 x 30 mL), and finally brine (1 x 30 mL). The organic extract was dried over sodium sulphate and evaporated. Pregnenolone acetate **6** was purified by column chromatography in silica gel with increasing hexane/ethyl acetate to afford 2.22 g of a white crystalline solid (isolated yield: 98%). NMR and HRMS shows that the product was pure and is consistent with that reported by literature [48].

4.2.2. Synthesis of 20-(*R*)-(prop-2-yn-1-yl)amino-5-pregnen-3β-ol acetate (C) and 20-(*S*)-(prop-2-yn-1-yl)amino-5-pregnen-3β-ol acetate (D)

To a solution of pregnenolone acetate (1.0 g, 2.80 mmol) in 20 mL of THF, propargylamine (0.93 g, 16.80 mmol), $NaBH(AcO)_3$ (1.18 g, 5.60 mmol) and finally 4 Å molecular sieves (100 mg) were added in this order and the reaction mixture was stirred at room temperature. Additional molecular sieves were added every 48 h until the reaction was completed in 1 week. Then, the reaction was quenched by addition of 5% $NaHCO_3$ (50 mL) and the layers were separated and filtered to remove the molecular sieves. The aqueous phase was extracted with ether (4x20 mL). Combined organic extracts were dried over Na_2SO_4 and concentrated. The products were purified by column chromatography in silica gel with increasing ethyl acetate/hexane gradient to yield a less polar fraction composed by **C**, 627

mg, 49% (light-yellow solid), and a more polar fraction containing **D**, 615 mg,48% (light-yellow solid).

4.2.2.1. 20-(*R*)-(prop-2-yn-1-yl)amino-5-pregnen-3β-ol acetate (C)

White solid. M.P.: 103.5 – 105.1 °C. Specific rotation [α] = -50.38 (c = 0.33 %, CH_2Cl_2). ^{1}H NMR (300 MHz, $CDCl_3$) δ 5.37 (d, 1H, *J* = 5.1 Hz, C6-H); 4.70 – 4.49 (m, 1H, C3-H); 3.49 (dd, 1H, *J* = 17.3, 2.5 Hz, NH-CH_2), 3.35 (dd, 1H, *J* = 17.2, 2.4 Hz, NH-CH_2); 2.84 (dd, 1H, *J* = 9.1, 6.0 Hz, C20-H); 2.31 (m, 2H, C4-H); 2.18 (t, 1H, *J* = 2.4 Hz, -C≡CH); 2.02 (s, 3H, -$COCH_3$); 2.01 – 1.91 (m, 2H); 1.85 (m, 3H); 1.69 – 1.40 (m, 9H); 1.31 (m, *J* = 6.1 Hz, 3H); 1.20 – 1.04 (m, 3H); 1.04 – 0.93 (m, 8H); 0.91 – 0.82 (m, 2H); 0.76 (s, 3H, C18-H). ^{13}C NMR (75 MHz, $CDCl_3$) δ 170.5 (C=O); 139.6 (C, C5); 122.5 (CH, C6); 82.6 (CH, ≡CH); 73.9 (CH, C3); 71.0 (C, -C≡); 56.3 (CH); 56.2 (CH); 53.8 (CH); 49.8 (CH); 42.0 (C); 40.2 (CH_2); 38.1 (CH_2); 37.0 (CH_2); 36.6 (C); 34.9 (-NH-CH_2); 31.8 (CH); 31.7 (CH_2); 27.7 (CH_2); 26.7 (CH_2); 24.1 (CH_2); 21.4 (CH_2); 21.0 (CH_2); 19.3 (CH_3); 18.5 (CH_2); 12.3 (CH_3). IR υ_{max} 3305 (≡C-H); 2942 (C-H); 1732 (C=O); 1453 (-CH_2-C≡) cm^{-1}. HRMS calculated mass for $C_{26}H_{40}NO_2$ ($M+H^+$) 398.3054; found m/z 398.3058.

4.2.2.2. 20-(*S*)-(prop-2-yn-1-yl)amino-5-pregnen-3β-ol acetate (D)

White solid. M.P.: 128.7 – 130.3 °C. Specific rotation [α] = -35.63 (c = 0.21 %, CH_2Cl_2). ^{1}H NMR (300 MHz, $CDCl_3$) δ 5.37 (d, 1H, *J* = 5.2 Hz, C6-H); 4.67 – 4.54 (m, 1H, C3-H); 3.48 (dd, 1H, *J* = 17.2, 2.5 Hz, NH-CH_2); 3.34 (dd, 1H, *J* = 17.2, 2.4 Hz, NH-CH_2); 2.75 (dd, 1H, *J* = 9.4, 6.1 Hz, C20-H); 2.32 (m, 2H, C4-H); 2.18 (t, 1H, *J* = 2.4 Hz, -C≡CH); 2.03 (s, 3H,-$COCH_3$); 2.01 – 1.76 (m, 5H); 1.52 (m, 10H); 1.38 – 1.11 (m, 4H); 1.11 – 0.88 (m, 9H); 0.72 (s, 3H, C18-H). ^{13}C NMR (75 MHz, $CDCl_3$) δ 170.5 (C=O); 139.7 (C, C5); 122.5 (CH, C6); 82.6 (CH, ≡CH); 73.9 (CH, C3); 71.0 (C, -C≡); 56.6 (CH); 56.3 (CH); 54.5 (CH); 49.9 (CH); 42.1 (C); 39.3 (CH_2); 38.1 (CH_2); 37.0 (CH_2); 36.6 (C); 35.1 (-NH-CH_2); 31.8 (CH); 31.7 (CH_2); 27.7 (CH_2); 26.9 (CH_2); 24.2 (CH_2); 21.4 (CH_2); 20.9 (CH_2); 19.3 (CH_3); 18.6 (CH_3); 12.3 (CH_3). IR υ_{max} 3268 (≡C-H); 2940 (C-H); 1733 (C=O); 1466 (-CH_2-C≡) cm^{-1}. HRMS calculated mass for $C_{26}H_{40}NO_2$ ($M+H^+$) 398.3054; found m/z 398.3058.

4.2.3. Synthesis of 3β-*t*-butyldimethylsilyloxy-5-pregnen-20-one (7)

Pregnenolone (2.00 g, 6.33 mmol) was dissolved in DMF (50 mL) at 0 °C. Then, imidazole (0.65 mg, 9.50 mmol) and 1.5 equivalents of TBDMS-Cl (1.43 g, 9.50 mmol) were successively added, and the mixture stirred at room temperature for 12 hours. Water was added (200 mL) and the solution was extracted with diethyl ether (3 x 100 mL). The combined organic phases were washed with brine (2 x 100 mL), dried over sodium sulphate, and evaporated. The product was purified by column chromatography in silica gel (isocratic, Hexane: EtOAc, 95:5). The product was obtained as a white solid (2.53 g, 93% yield). M.P.: 156.7 – 158.6 °C. Specific rotation [α] = +18.39 (c = 0.37 %, CH_2Cl_2). ^{1}H NMR (300 MHz, $CDCl_3$) δ 5.31 (d, 1H, *J* = 5.2 Hz, C6-H); 3.48 (m, 1H, C3-H); 2.52 (t, 1H, *J* = 8.8 Hz, C17-H); 2.12 (m, 6H); 2.03 (m, 2H); 1.91 – 1.34 (m, 11H); 1.33-0.94 (m, 7H); 0.88 (s, 9H, Si-C$(CH_3)_3$); 0.62 (s, 3H, C18-H); 0.05 (s, 6H, Si-CH_3). ^{13}C NMR (75 MHz, $CDCl_3$) δ 209.6 (C=O), 141.5 (C5), 120.9 (C6), 72.5 (C3), 63.7 (C17), 57.0 (C14), 50.1 (C9), 44.0 (C13), 42.8 (CH_2), 38.9 (CH_2), 37.4 (CH_2), 36.6 (C10), 32.0 (CH_2), 31.9 (CH_2), 31.8 (CH_2), 31.5 (C21), 25.9 (Si-C$(CH_3)_3$), 24.5 (CH_2), 22.8 (CH_2), 21.1 (CH_2), 19.4 (C19), 18.3 (Si-C-), 13.2 (C18), -4.6 (Si-CH_3). IR υ_{max} 2955 (C-H); 1700 (C=O); 1243 (Si-CH_3). HRMS calculated mass for $C_{27}H_{47}O_2Si$ ($M+H^+$) 431.3334; found m/z 431.3355. Spectral data shows that the product was pure and is consistent with that reported by literature [49].

4.2.4. Synthesis of 3β-(*t*-butyldimethylsilyloxy)-20-methylpregn-5-en-20*R*,21-epoxide (8)

NaH (336 mg, 14 mmol) were dissolved in DMSO (50 mL) and trimethylsulfonium iodide (1.44 g, 18.64 mmol) were added. The mixture was vigorously stirred for 2 hours at room temperature. Then, **7** (2.00 g, 4.66 mmol) was added. After 18 hours at room temperature, water was added to the mixture. The solution was extracted with diethyl ether (3 x 100 mL). The combined organic phases were washed successively with water (2 x 100 mL) and brine (1 x 100 mL), dried over sodium sulphate and evaporated. The product was purified by column chromatography in silica gel (in gradient, using hexane and ethyl acetate). The product was obtained as a white solid (1.88 g, 91% yield). M.P.: 127.3 – 129.5 °C. Specific rotation [α] = -38.85 (c = 0.17 %, CH_2Cl_2). ^{1}H NMR (300 MHz, $CDCl_3$) δ 5.31 (d, 1H, *J* = 5.1

Hz, C6-H); 3.48 (dt, 1H, *J* = 11.0, 5.6 Hz, C3-H); 2.50 (d, 1H, *J* = 4.9 Hz, O-CH_2); 2.32 (d, 1H, *J* = 5.0 Hz, O-CH_2); 2.28 – 1.88 (m, 4H); 1.88 – 1.33 (m, 15H); 1.33 – 0.96 (m, 8H); 0.89 (s, 9H, Si-C(CH_3)$_3$); 0.81 (s, 3H, C18); 0.05 (s, 6H, Si-CH_3). ^{13}C NMR (75 MHz, CDCl3) δ 141.6 (C, C5); 121.0 (CH, C6); 72.6 (CH, C3); 56.7 (CH, C14); 56.1 (C); 54.2 (CH); 51.6 (CH_2, C22); 50.1 (CH, C9); 44.0 (C); 42.8 (CH_2); 39.5 (CH_2); 37.4 (CH_2); 36.6 (C); 32,0 (CH_2); 31.7 (CH_2); 31.8 (CH_2); 25,9 (CH_3, C(CH_3)$_3$), 23.8 (CH_2); 22.6 (CH_3); 21.8 (CH_2); 20:9 (CH_2); 19.4 (CH_3); 18,3 (C, Si-C-); 13.0 (CH_3); -4,6 (CH_3, Si-CH_3). IR υ_{max} 3040 (=C-H), 2933 (-C-H), 2955 (C-H); 1230 (Si-CH_3), 940 (C-O). HRMS calculated mass for $C_{28}H_{49}O_2Si$ ($M+H^+$) 445.3496; found m/z 445.3485. Spectral data shows that the product was pure and is consistent with that reported by literature [50].

4.2.5. Synthesis of 3β-(*t*-butyldimethylsilyloxy)-20-(*R*)-(prop-2-yn-1-yl)aminomethyl-5-pregnen-20-ol (9)

Epoxide **8** (900 mg, 2.02 mmol) was dissolved in CH_3CN (30 mL). $LiClO_4$ (6.45 g, 60 mmol) and propargyl bromide (1.20 g, 10.1 mmol) were slowly added at room temperature. Then the mixture was heated until boiling for 5 days. Finally, water (100 mL) was added and the solution was extracted with DCM (3 x 30 mL). The combined organic phases were dried with sodium sulphate and evaporated. The product was purified by chromatography in a silica gel column (in gradient, Hexane-AcOEt). The product was obtained as a light-yellow solid (881 mg, 87% yield). M.P.: 140.8 – 142.7 °C. Specific rotation [α] = -37.80 (c = 0.34 %, CH_2Cl_2). ^{1}H NMR (300 MHz, $CDCl_3$) δ 5.31 (d, 1H, *J* = 5.0 Hz, C6-H); 3.56 – 3.35 (m, 3H, NH-CH_2, C3-H); 2.59 (s, 2H, C22-H); 2.22 (t, 1H, *J* = 2.4 Hz, ≡CH); 2.37 – 1.90 (m, 4H); 1.90 – 1.33 (m, 16H); 1.24 (s, 6H); 1.00 (m, 5H); 0.89 (s, 9H, *J* = 0.9 Hz, SiC(CH_3)$_3$); 0.85 (s, 3H, C18-H); 0.06 (s, 6H, Si-CH_3). ^{13}C NMR (75 MHz, $CDCl_3$) δ 141.6 (C, C5); 121.1 (CH, C6); 82.2 (CH, ≡CH); 73.4 (CH, C3); 72.6 (C, C20); 71.3 (C, -C≡); 58.7 (CH_2); 57.5 (CH); 57.0 (CH); 50.2 (CH); 42.8 (C) ; 42.7 (CH_2); 40.1 (C); 39.0 (CH_2); 37.4 (CH_2); 36.6 (C); 32.1 (CH_2); 31.8 (CH); 31.4 (CH_2); 25.9 (CH_3, C(CH_3)$_3$); 25.1 (CH_3); 23.9 (CH_2); 22.5 (CH_2); 20.9 (CH_2); 19.4 (CH_3); 18.3 (Si-C); 13.5 (CH_3); -4.6 (Si-CH_3). IR υ_{max} 3443 (O-H), 3308 (≡C-H); 2942 (C-H); 1240 (Si-C). HRMS calculated mass for $C_{31}H_{54}NO_2Si$ ($M+H^+$) 500.3918; found m/z 500.3930.

4.2.6. Synthesis of 20-(*R*)-(prop-2-yn-1-yl)aminomethyl-5-pregnen-3β,20-diol (E)

Terminal alkyne intermediate **9** (800 mg, 1.60 mmol) was dissolved in THF (30 mL). A solution 1M TBAF in THF (3.20 mL) was slowly added, at room temperature and stirred overnight. Water (100 mL) was added, and the solution was extracted with diethyl ether (3 x 30 mL). Combined organic phases were washed with water (2 x 50 mL), dried over sodium sulphate and evaporated. The product was purified by chromatographic column in silica gel (in gradient, hexane-EtOAc). The product was obtained as a white solid (555 mg, 90% yield). M.P.: 151.7 – 153.9 °C. Specific rotation [α] = -55.70 (c = 0.11 %, CH_2Cl_2). ^{1}H NMR (300 MHz, $CDCl_3$) δ 5.35 (d, 1H, *J* = 5.1 Hz, 1H); 3.63 – 3.38 (m, 3H, NH-CH_2, C3-H); 2.59 (s, 2H, C22-H); 2.22 (t, 1H, *J* = 2.4 Hz, ≡CH); 2.17 – 1.58 (m, 15H); 1.49 (m, 8H); 1.23 (m, 8H), 0.96 (m, 9H), 0.86 (s, 3H, C18-H). ^{13}C NMR (75 MHz, $CDCl_3$) δ 140.8 (C, C5); 121.5 (CH, C6); 82.5 (CH, ≡CH); 72.5 (C, C20); 71.7 (C, -C≡); 71.0 (CH, C3); 58.6 (CH_2); 57.4 (CH); 56.1 (CH); 53.8 (CH); 49.9 (CH); 42.3 (C); 42.1 (CH_2); 40.3 (C); 39.2 (CH_2); 36.5 (C); 32.9 (CH_2); 31.8 (CH); 31.6 (CH_2); 25.1 (CH_3); 24.1 (CH_3); 21.1 (CH_2); 19.4 (CH_3); 18.4 (CH_3); 13.3 (CH_3). IR υ_{max} 3480 (O-H), 3305 (≡C-H); 2930 (C-H); 1453 (-CH_2-C≡). HRMS calculated mass for $C_{25}H_{40}NO_2$ ($M+H^+$) 386.3054; found m/z 386.3038.

4.2.7. Synthesis of 3β-(*t*-butyldimethylsilyloxy)-20-(*R*)-azidomethyl-5-pregnen-20-ol (10)

Epoxide **8** (900 mg, 2.02 mmol) was dissolved in CH_3CN (30 mL). $LiClO_4$ (9.70 g, 91 mmol) and NaN_3 (1.31 g, 20.2 mmol) were slowly added at room temperature. Then the mixture was heated until boiling for 5 days. Finally, water (100 mL) was added, and the solution was extracted with DCM (3 x 30 mL). The combined organic phases were dried with sodium sulphate and evaporated. The product was purified by chromatography in a silica gel column (isocratic, 95% Hexane-5% AcOEt). The product was obtained as a white solid (691 mg, 70% yield). M.P.: 123.9 – 126.0 °C. Specific rotation [α] = -38.43 (c = 0.12 %, CH_2Cl_2). ^{1}H NMR (300 MHz, $CDCl_3$) δ 5.31 (d, 1H, *J* = 5.2 Hz, C6–H); 3.48 (q, 1H, *J* = 5.2 Hz, C3–H); 3.30 (d, 1H, *J* = 12.0 Hz, N_3-CH_2); 3.11 (d, 1H, *J* = 12.0 Hz, N_3-CH_2); 2.20 (m, 2H; C4–H); 2.06-1.45 (m, 15H); 1.34-0.98 (m, 6H); 0.89 (s, 9H, $C(CH_3)_3$); 0.84 (s, 3H, C18–H); 0.06 (s, 6 H, Si-CH_3). ^{13}C NMR (75 MHz, $CDCl_3$) δ 141.6 (C, C5); 121.0 (CH, C6); 75.2 (C, C20); 72.6 (CH,

C3); 61.5 (CH_2, C22); 56.8 (CH); 56.2 (CH); 50.0 (CH); 42.8 (C); 42.7 (CH_2); 39.9 (CH_2); 37.4 (CH_2); 36.6 (C); 32.1 (CH_2); 31.8 (CH_2); 31.3 (CH); 25.9 (CH_3, $C(CH_3)_3$); 24.9 (CH_3); 23.8 (CH_2); 22.3 (CH_2); 20.9 (CH_2); 19.4 (CH_3); 18.3 (C, Si-C-); 13.6 (CH_3); -4,6 (CH_3, Si-CH_3). IR υ_{max} 3420 (O-H), 2951 (-C-H), 2050 (-N_3), 1221 (Si-C). HRMS calculated mass for $C_{28}H_{50}N_3O_2Si$ ($M+H^+$) 488.3667; found m/z 488.3674.

4.2.8. Synthesis of 20-(*R*)-azidomethyl-5-pregnen-3β,20-diol (F)

Azide intermediate **10** (800 mg, 1.64 mmol) was dissolved in THF (30 mL). A solution 1M TBAF in THF (3.28 mL) was slowly added, at room temperature and stirred overnight. Water (100 mL) was added, and the solution was extracted with diethyl ether (3 x 30 mL). Combined organic phases were washed with water (2 x 50 mL), dried over sodium sulphate, and evaporated. The product was purified by chromatographic column in silica gel (in gradient, hexane-EtOAc). The product was obtained as a white solid (533 mg, 87% yield). M.P.: 164.5 – 166.3 °C. Specific rotation [α] = -47.38 (c = 0.16 %, CH_2Cl_2). ^{1}H NMR (300 MHz, $CDCl_3$) δ 5.35 (d, 1H, *J* = 5.0 Hz, C6–H); 3.48 (q, 1H, *J* = 5.2 Hz, C3–H); 3.22 (d, 1H, *J* = 12.0 Hz, N_3-CH_2); 3.18 (d, 1H, *J* = 12.0 Hz, N_3-CH_2); 2,23 (m, 2H; C4–H); 2.06-1.38 (m, 15H); 1.34 (s, 3H, C21–H); 1-32-0.98 (m, 9H); 0.84 (s, 3H, C18–H). ^{13}C NMR (75 MHz, $CDCl_3$) δ 140.8 (C, C5); 121.5 (CH, C6); 75.2 (C, C20); 71.7 (CH, C3); 61.5 (CH_2, C22); 56.7 (CH); 56.2 (CH); 50.0 (CH); 42.8 (C); 42.3 (CH_2); 39.9 (CH_2); 37.2 (CH_2); 36.5 (C); 31.9 (CH_2); 31.7 (CH_2); 31.2 (CH); 24.9 (CH_3); 23.8 (CH_2); 22.3 (CH_2); 20.9 (CH_2); 19.4 (CH_3); 13,2 (CH_3). IR υ_{max} 3407 (O-H), 2932 (-C-H), 2053 (-N_3). HRMS calculated mass for $C_{22}H_{36}N_3O_2$ ($M+H^+$) 374.2802; found m/z 374.2806.

4.2.9. General procedure for the Cu(I) mediated 1,3-dipolar azide alkyne cycloaddition reaction (CuAAC).

Alkyne (1 equivalent) and azide (1.2 equivalent) were suspended in 10 mL/eq of t-BuOH:H_2O (1:1). Then, 1 M CuSO4 solution (0.05 equivalents) and 1 M sodium ascorbate solution (0.2 equivalents) were added, and the mixture stirred overnight at room temperature. Brine (30 mL) was added, and the solution was extracted with dichloromethane (3 x 25 mL). Combined organic extracts were dried over sodium sulphate and evaporated. Products were purified by column chromatography in silica gel with increasing hexane/ethyl acetate or dichloromethane/methanol gradients.

4.2.9.1. Synthesis of 20-(*R*)-((1-benzyl-*1H*-1,2,3-triazol-4-yl)methyl)amino-5-pregnen-3β-ol acetate (C1)

Following the general reaction conditions for CuAAC reaction, the reaction was worked up and purified to afford 60 mg of a yellow solid (isolated yield: 90%). M.P.: 157.8 – 159.9 °C (decomposition). Specific rotation [α] = -44.99 (c = 0.42 %, CH_2Cl_2). ^{1}H NMR (300 MHz, $CDCl_3$) δ 7.36 (s, 1H, $C5_{triazole}$-H); 7.35 (m, 3H, *p*- and *m*-aromatics); 7.26 (m, 2H, *o*-aromatics); 5.50 (s, 2H, CH_2-phenyl); 5.36 (d, 1H, *J* = 5.1 Hz, C6-H); 4.71 – 4.49 (m, 1H, C3-H); 3.97 (d, 1H, *J* = 13.7 Hz, NH-CH_2); 3.74 (d, 1H, *J* = 13.7 Hz, NH-CH_2); 2.62 (m, 1H, C20-H); 2.31 (d, 2H, *J* = 7.8 Hz, C4-H); 2.03 (s, 3H, $COCH_3$); 2.01 – 1.68 (m, 8H); 1.68 – 1.14 (m, 11H); 1.15 – 0.88 (m, 11H); 0.88 – 0.72 (m, 2H); 0.60 (s, 3H, C18-H). ^{13}C NMR (75 MHz, $CDCl_3$) δ 170.5 (C=O); 147.5 (C, $C4_{triazole}$); 139.7 (C, C5); 134.8 (C, ipso-aromatic); 129.1 (CH, m-aromatic); 128.7 (C, p-aromatic); 128.0 (CH, *o*-aromatic); 122.5 (CH, C6); 121.5 (CH, $C5_{triazole}$); 73.9 (CH, C3); 56.3 (CH); 56.1 (CH); 55.1 (CH); 54.1 (CH2, CH_2-phenyl); 49.9 (CH); 42.1 (CH_2, NH-CH_2); 41.7 (C); 40.0 (CH_2); 38.1 (CH_2); 37.0 (CH_2); 36.6 (C); 31.8 (CH_2); 31.7 (CH); 27.8 (CH_2); 26.7 (CH_2); 24.1 (CH_2); 21.4 (CH_2); 21.0 (CH_2); 19.3 (CH_3); 19.0 (CH_3); 12.2 (CH_3). IR υ_{max} 3347 (N-H), 3025 (=C-H), 2937 (-C-H), 2833 (-C-H), 1740 (C=O), 1663 cm^{-1}. HRMS calculated mass for $C_{33}H_{47}N_4O_2$ ($M+H^+$) 531.3694; found m/z 531.3690.

4.2.9.2. Synthesis of 20-(*R*)-((1-(2-ethoxy-2-oxoethan-1-yl)-*1H*-1,2,3-triazol-4-yl)methyl)amino-5-pregnen-3β-ol acetate (C2)

Following the general reaction conditions for CuAAC reaction, the reaction was worked up and purified to afford 57 mg of a light-yellow solid (isolated yield: 86%). M.P.: 119.3 – 121.2 °C. Specific rotation [α] = -36.54 (c = 0.54 %, CH_2Cl_2). ^{1}H NMR (300 MHz, $CDCl_3$) δ 7.59 (s, 1H, $C5_{triazole}$-H); 5.32 (d, 1H, *J* = 5.0 Hz, C6-H); 5.13 (s, 2H, -CH_2-COOEt); 4.59 (m, 1H, C3-H); 4.25 (q, 2H, *J* = 7.1 Hz, -C(O)O-CH_2-); 4.04 (d, 1H, *J* = 13.8 Hz, NH-CH_2); 3.80 (d, 1H, *J* = 13.8 Hz, NH-CH_2); 2.67 (m, 1H, C20-H); 2.39 – 2.16 (m, 2H, C4-H); 2.03 – 1.91 (m, 3H); 2.01 (s, 3H, $COCH_3$) 1.91 – 1.67 (m, 4H); 1.47 (s, 8H); 1.29 (m, 7H); 1.16 – 0.81 (m, 12H); 0.65 (s, 3H, C18-H). ^{13}C NMR (75 MHz, $CDCl_3$) δ 170.5 (C=O); 166.3 (C=O); 147.4 (C, $C4_{triazole}$); 140.8 (C, C5); 123.0 (CH, $C5_{triazole}$); 121.5 (CH, C6); 73.7 (CH, C3); 62.4 (CH_2, -OCH_2-); 56.4 (CH); 56.1 (CH); 55.1 (CH); 50.9 (CH_2, $N1_{triazole}$-CH_2); 50.0 (CH); 42.3 (CH_2); 42.1 (C); 41.6 (CH_2, NH-CH_2); 40.0 (CH_2);

37.2 (CH_2); 36.5 (C); 31.8 (CH_2); 31.8 (CH_2); 31.7 (CH_2); 26.8 (CH_2); 24.2 (CH_2); 21.1 (CH_2); 19.4 (CH_3); 18.9 (CH_3); 14.1 (CH_3, O-CH_2-CH_3); 12.2 (CH_2, C18-H). IR υ_{max} 3335 (N-H), 3033 (=C-H), 2940 (-C-H), 1750 (C=O),1740 (C=O) cm^{-1}. HRMS calculated mass for $C_{30}H_{47}N_4O_4$ ($M+H^+$) 527.3592; found m/z 527.3598.

4.2.9.3. Synthesis of 20-(*R*)-((1-octyl-*1H*-1,2,3-triazol-4-yl)methyl)amino-5-pregnen-3β-ol acetate (C3)

Following the general reaction conditions for CuAAC reaction, the reaction was worked up and purified to afford 53 mg of a yellow oil (isolated yield: 76%). Specific rotation [α] = -40.77 (c = 0.50 %, CH_2Cl_2). ^{1}H NMR (300 MHz, $CDCl_3$) δ 7.41 (s, 1H, $C5_{triazol}$e-H); 5.34 (d, 1H, *J* = 5.0 Hz, C6-H); 4.68 – 4.47 (m, 1H, C3-H); 4.30 (t, 2H, *J* = 7.2 Hz, N1triazole-CH_2); 3.98 (d, 1H, *J* = 13.6 Hz, NH-CH_2-); 3.75 (d, 1H, *J* = 13.6 Hz; NH-CH_2-); 2.63 (dd, 1H, *J* = 9.4, 6.1 Hz, C20-H); 2.29 (m, 2H, *J* = 7.4 Hz, C4-H); 2.00 (s, 3H, $COCH_3$); 1.99 – 1.68 (m, 10H); 1.47 (m, 7H); 1.26 (m, 14H, -CH_2-); 1.17 – 0.90 (m, 11H); 0.90 – 0.79 (m, 4H); 0.63 (s, 3H, C18-H). ^{13}C NMR (75 MHz, $CDCl_3$) δ 170.5 (C=O); 147.0 (C, $C4_{triazole}$); 139.6 (C, C5); 122.5 (CH, C6); 121.3 (CH, $C5_{triazole}$); 73.9 (CH, C3); 56.3 (CH); 56.2 (CH); 55.2 (CH); 50.2 (CH_2, $N1_{triazole}$-CH_2); 49.9 (CH); 42.1 (C); 41.8 (CH_2, NH-CH_2); 40.0 (CH_2); 38.1 (CH_2); 37.0 (CH_2); 36.6 (C); 31.8 (CH_2); 31.7 (CH_2); 31.7 (CH_2); 30.3 (CH_2); 29.1 (CH_2); 29.0 (CH_2); 27.7 (CH_2); 26.8 (CH_2); 26.5(CH_2) ; 24.1 (CH_2); 22.6 (CH_2); 21.4 (CH_2); 21.1 (CH_2); 19.3 (CH_3); 19.0 (CH_3); 14.1 (CH_2, heptyl-CH_2); 12.2 (CH_3). IR υ_{max} 3430 (N-H); 3021(=C-H), 2924 (-C-H), 2850 (-C-H), 1750 (C=O), 1631 (-C=C-), 1456 cm^{-1}. HRMS calculated mass for $C_{34}H_{57}N_4O_2$ ($M+H^+$) 553.4476; found m/z 553.4473.

4.2.9.4. Synthesis of 20-(*R*)-((1-(3,7-dimethylocta-2,6-dien-1-yl)-*1H*-1,2,3-triazol-4-yl)methyl)amino-5-pregnen-3β-ol acetate (C4)

Following the general reaction conditions for CuAAC reaction, the reaction was worked up and purified to afford 58 mg of a yellow oil (isolated yield: 80%). Specific rotation [α] = -40.30 (c = 0.58 %, CH_2Cl_2). ^{1}H NMR (300 MHz, $CDCl_3$) δ 7.39 (s, 1H, $C5_{triazole}$*E*-H); 7.38 (s, 1H, $C5_{triazole}$*Z*-H); 5.39 (m, 1H, -CH=C); 5.34 (d, 1H, *J* = 5.0 Hz, C6–H) 5.15 – 5.00 (m, 1H, -CH=C); 4.91 (t, 2H, *J* = 6.7 Hz,

$N1_{triazole}$-CH2-); 4.57 (m, 1H, C3-H); 3.96 (d, 1H, *J* = 13.5 Hz, NH-CH_2-); 3.73 (d, 1H, *J* = 13.5 Hz, NH-CH_2-); 2.64 (m, 1H, C20-H); 2.29 (d, 2H, *J* = 7.3 Hz, C4-H); 2.04 (m, 9H); 2.01 (s, 3H, $COCH_3$); 1.89 – 1.63 (m, 11H); 1.63 – 1.12 (m, 25H); 1.12 – 0.91 (m, 14H); 0.91 – 0.74 (m, 6H); 0.64 (s, 3H, C18-H). ^{13}C NMR (75 MHz, $CDCl_3$) δ 170.5 (C=O); 147.1 (C, $C4_{triazole}$); 143.0 (C, C=CH); 142.8 (C, C=CH); 139.6 (C, C5); 132.6 (C, C=CH); 132.1 (C, C=CH); 130.9 (CH, C=CH); 128.8 (CH, C=CH); 123.4 (CH, C=CH); 122.5 (CH, C6); 120.8 (CH, $C5_{triazole}$); 118.0 (CH, C=CH); 117.1 (CH, C=CH); 73.9 (CH, C3); 56.3 (CH); 56.2 (CH); 55.2 (CH); 49.9 (CH); 47.8 (CH_2, $N1_{triazole}$-CH_2-); 42.1 (CH_2, $N1_{triazole}$-CH_2-); 41.8 (CH_2, NH-CH_2); 40.0 (CH_2); 39.4 (CH_2); 38.1 (CH_2); 36.9 (CH_2); 36.6 (C); 31.8 (CH_2); 31.7 (CH_2); 26.8 (CH_2); 26.2 (CH_2); 25.7 (CH_3); 24.1 (CH_2); 23.4 (CH_3); 21.4 (CH_2); 21.0 (CH_2); 19.3 (CH_3); 19.1 (CH_3); 19.0 (CH_3); 17.7 (CH_3); 16.4 (CH_3); 12.2 (CH_3). IR υ_{max} 3380 (N-H), 3055 (=C-H), 2954 (-C-H), 1744 (C=O), 1451 cm^{-1}. HRMS calculated mass for $C_{36}H_{57}N_4O_2$ ($M+H^+$) 577.4476; found m/z 577.4479.

4.2.9.5. Synthesis of 20-(*R*)-((1-(3-phenylpropyl)-*1H*-1,2,3-triazol-4-yl)methyl)amino-5-pregnen-3β-ol acetate (C5)

Following the general reaction conditions for CuAAC reaction, the reaction was worked up and purified to afford 60 mg of a yellow oil (isolated yield: 85%). Specific rotation [α] = -36.91 (c = 0.38 %, CH_2Cl_2). ^{1}H NMR (300 MHz, $CDCl_3$) δ 7.49 (s, 1H, $C5_{triazole}$-H); 7.36 – 7.24 (m, 2H, *m*-aromatic); 7.24 – 7.09 (m, 3H, *p*- and *o*-aromatic); 5.40 – 5.30 (m, 1H, C6-H); 4.69 – 4.51 (m, 1H, C3-H); 4.32 (t, 2H, *J* = 7.1 Hz, $N1_{triazole}$-CH_2-); 4.01 (d, 1H, *J* = 13.7 Hz, NH-CH_2-); 3.81 (d, 1H, *J* = 13.6 Hz, NH-CH_2-); 2.63 (t, 2H, J = 7.5 Hz, CH_2-phenyl); 2.57 (m, 1H, C20-H); 2.38 – 2.11 (m, 4H); 2.01 (s, 3H, $COCH_3$); 1.84 (m, 5H); 1.73 – 1.29 (m, 9H); 1.29 – 0.80 (m, 13H); 0.65 (s, 3H, C18-H). ^{13}C NMR (75 MHz, $CDCl_3$) δ 170.5 (C=O); 146.5 (C, $C4_{triazole}$); 140.2 (C, ipso-aromatic); 139.6 (C, C5); 128.6 (CH, *m*-aromatic); 128.4 (CH, *o*-aromatic); 126.3 (CH, *p*-aromatic); 122.5 (CH, C6); 121.8 (CH, $C5_{triazole}$); 73.9 (CH, C3); 56.5 (CH); 56.1 (CH); 55.9 (CH); 49.9 (CH); 49.5 (CH_2-phenyl); 42.0 (CH_2); 41.4 (NH-CH_2); 39.2 (CH_2); 38.1 (CH_2); 37.0 (CH_2); 36.6 (C); 32.5 ($N1_{triazole}$-CH_2); 31.8 (CH_2); 31.7 (CH_2); 27.7 (CH_2); 27.1 (CH_2); 24.1 (CH_2); 21.4 (CH_2); 20.9 (CH_2); 19.3 (CH_3); 18.8 (CH_3); 12.2 (CH_3). IR υ_{max} 3400 (N-H), 3015

(=C-H), 2862 (-C-H), 1750 (C=O), 1451 cm^{-1}. HRMS calculated mass for $C_{35}H_{51}N_4O_2$ ($M+H^+$) 559.4007; found m/z 559.4012.

4.2.9.6. Synthesis of 20-(*S*)-((1-benzyl-*1H*-1,2,3-triazol-4-yl)methyl)amino-5-pregnen-3β-ol acetate (D1)

Following the general reaction conditions for CuAAC reaction, the reaction was worked up and purified to afford 55 mg of an off-white solid (isolated yield: 83%). M.P.: 60.7 – 62.6 °C. Specific rotation [α] = -19.03 (c = 0.11 %, CH_2Cl_2). ^{1}H NMR (300 MHz, $CDCl_3$) δ 7.76 (s, 1H, $C5_{triazole}$-H); 7.32 (m, 3H, *p*- and *m*-aromatics); 7.23 (m, 2H, *o*-aromatics); 5.50 (s, 2H, CH_2–phenyl); 5.34 (d, 1H, *J* = 4.1 Hz, C6-H); 4.57 (m, 1H, C3-H); 4.18 (d, 1H, *J* = 13.8 Hz, NH-CH_2); 3.97 (d, 1H, *J* = 13.8 Hz, NH-CH_2); 2.78 (dd, 1H, *J* = 10.3, 6.2 Hz, C20-H); 2.30 (d, 2H, *J* = 7.5 Hz, C4-H); 2.01 (s, 3H, CH_3CO-); 1.98 – 1.71 (m, 7H); 1.71 – 1.34 (m, 7H); 1.35 – 0.72 (m, 13H); 0.59 (s, 3H, C18-H). ^{13}C NMR (75 MHz, $CDCl_3$) δ 170.5 (C=O); 143.1 (C, $C4_{triazole}$); 139.6 (C, C5); 134.6 (C, ipso-aromatic); 129.1 (CH, p-aromatic); 128.7 (CH, m-aromatic); 128.0 (CH, o-aromatic); 123.7 (CH, $C5_{triazole}$); 122.3 (CH, C6); 73.9 (CH, C3); 56.3 (CH); 55.9 (CH); 54.5 (CH); 54.2 (CH2, CH_2–phenyl); 49.8 (CH); 42.3 (CH_2); 39.6 (CH_2); 39.1 (CH_2); 38.0 (CH_2); 36.9 (C); 36.5 (C); 31.7 (CH_2); 31.6 (CH); 27.7 (CH_2); 27.0 (CH_2); 24.2 (CH_2); 21.4 ($COCH_3$); 20.8 (CH_2); 19.3 (CH_3); 17.2 (CH_3); 12.0 (CH_3). IR υ_{max} 3340 (N-H), 3014 (=C-H), 2940(-C-H), 2878 (-C-H), 1757 (C=O), 1689 cm^{-1}. HRMS calculated mass for $C_{33}H_{47}N_4O_2$ ($M+H^+$) 531.3694; found m/z 531.3694.

4.2.9.7. Synthesis of 20-(*S*)-((1-(2-ethoxy-2-oxoethan-1-yl)-*1H*-1,2,3-triazol-4-yl)methyl)amino-5-pregnen-3β-ol acetate (D2)

Following the general reaction conditions for CuAAC reaction, the reaction was worked up and purified to afford 46 mg of a white solid (isolated yield: 70%). M.P.: 90.0 – 91.9 °C. Specific rotation [α] = -17.56 (c = 0.34 %, CH_2Cl_2). ^{1}H NMR (300 MHz, $CDCl_3$) δ 7.61 (s, 1H, $C5_{triazole}$-H); 5.36 (d, 1H, *J* = 5.0 Hz, C6-H); 5.12 (d, 2H, *J* = 1.3 Hz, -CH2-COOEt); 4.59 (m, 1H, C3-H); 4.25 (q, 2H, *J* = 7.1 Hz, O-CH_2-); 4.01 (d, 1H, *J* = 13.8 Hz, NH-CH_2-); 3.82 (d, 1H, *J* = 13.8 Hz, NH-CH_2-); 2.60 (m, 1H, C20-H); 2.30 (m, 2H, C4-H); 2.22 – 1.74 (m, 9H); 2.01 (s, 3H, -$COCH_3$) 1.73 –

1.23 (m, 13H); 1.23 – 0.86 (m, 12H); 0.66 (s, 3H, C18-H). ^{13}C NMR (75 MHz, $CDCl_3$) δ 170.5 (C=O); 166.3 (C=O); 147.4 (C, $C4_{triazole}$); 139.6 (C, C5); 123.1 (CH, $C5_{triazole}$); 122.5 (CH, C6); 73.9 (CH, C3); 62.4 (CH_2, -OCH_2-); 56.5 (CH); 56.3 (CH); 55.9 (CH); 50.9 (CH2, $N1_{triazole}$-CH_2-); 49.9 (CH); 42.0 (CH_2); 41.5 (NH-CH_2); 39.2 (CH_2); 38.1 (CH_2); 37.0 (CH_2); 36.6 (C); 31.8 (CH_2); 31.7 (CH_2); 27.7 (CH_2); 27.1 (CH_2); 24.1 (CH_2); 21.4 (CH_2); 20.9 (CH_2); 19.3 (CH_3); 19.0 (CH_3); 14.1 (CH_3, O-CH_2-CH_3); 12.2 (CH_3). IR υ_{max} 3401 (N-H), 3045 (=C-H), 2986 (-C-H), 1754 (C=O),1745 (C=O) cm^{-1}. HRMS calculated mass for $C_{30}H_{47}N_4O_4$ ($M+H^+$) 527.3592; found m/z 527.3595.

4.2.9.8. Synthesis of 20-(*S*)-((1-octyl-*1H*-1,2,3-triazol-4-yl)methyl)amino-5-pregnen-3β-ol acetate (D3)

Following the general reaction conditions for CuAAC reaction, the reaction was worked up and purified to afford 56 mg of a white solid (isolated yield: 81%). M.P.: 105.3 – 107.1 °C. Specific rotation [α] = -17.49 (c = 0.14 %, CH_2Cl_2). ^{1}H NMR (300 MHz, $CDCl_3$) δ 7.79 (s, 1H, $C5_{triazole}$-H); 5.34 (d, 1H, *J* = 4.9 Hz, C6-H); 4.58 (dd, *J* = 6.5, 4.1 Hz, 1H, C3-H); 4.32 (t, *J* = 7.2 Hz, 2H, $N1_{triazole}$-CH_2-); 4.22 (d, 1H, *J* = 13.8 Hz, NH-CH_2); 3.99 (d, *J* = 13.8 Hz, 1H, NH-CH_2); 2.81 (m, 1H, C20-H); 2.30 (m, 2H, C4-H); 2.01 (s, 3H, $COCH_3$); 2.00 – 1.74 (m, 10H); 1.74 – 1.37 (m, 8H); 1.37 – 1.13 (m, 18H); 0.99 (m, 4H); 0.83 (t, 3H,*J* = 6.6 Hz, heptyl-CH3); 0.62 (s, 3H, C18-H). ^{13}C NMR (75 MHz, $CDCl_3$) δ 170.5 (C=O); 139.6 (C, $C4_{triazole}$); 139.6 (C, C5); 123.0 (CH, $C5_{triazole}$); 122.4 (CH, C6); 73.9 (CH, C3); 56.4 (CH); 56.0 (CH); 54.9 (CH); 50.4 (CH2, $N1_{triazole}$-CH_2-); 49.8 (CH_2); 42.2 (C); 40.2 (NH-CH_2); 39.1 (CH_2); 38.1 (CH_2); 37.0 (CH_2); 36.5 (C); 31.7 (CH_2); 30.3 (CH_2); 29.1 (CH_2); 29.0 (CH_2); 27.7 (CH_2); 27.1 (CH_2); 26.5 (CH_2); 24.2 (CH_2); 22.6 (CH_2); 21.4 (CH_2); 20.8 (CH_2); 19.3 (CH_3); 17.7 (CH_3); 14.1 (heptyl-CH_3); 12.1 (CH_3). IR υ_{max} 3404 (N-H); 3011(=C-H), 2958 (-C-H), 1748 (C=O), 1615, 1458 cm^{-1}. HRMS calculated mass for $C_{34}H_{57}N_4O_2$ ($M+H^+$) 553.4476; found m/z 553.4475.

4.2.9.9. Synthesis of 20-(*S*)-((1-(3,7-dimethylocta-2,6-dien-1-yl)-*1H*-1,2,3-triazol-4-yl)methyl)amino-5-pregnen-3β-ol acetate (D4)

Following the general reaction conditions for CuAAC reaction, the reaction was worked up and purified to afford 64 mg of a white solid (isolated yield: 88%). M.P.: 74.2 – 76.0 °C. Specific rotation [α] = -15.11 (c = 0.32 %, CH_2Cl_2). ^{1}H NMR (300 MHz, $CDCl_3$) δ 7.70 (s, 1H, $C5_{triazole}$-H); 5.38 (t, 1H, *J* = 7.3 Hz, $N1_{triazole}$-CH_2-CH=C); 5.34 (d, 1H, *J* = 4.9 Hz, C6-H); 5.19 – 4.95 (m, 1H, CH=C); 4.91 (7, *J* = 7.0 Hz, 2H, $N1_{triazole}$-CH_2-); 4.57 (m, 1H, C3-H); 4.16 (d, 1H, *J* = 13.8 Hz, NH-CH_2-); 3.95 (d, 1H, *J* = 13.7 Hz, NH-CH_2-); 2.78 (dd, 1H, *J* = 10.3, 6.1 Hz, C20-H); 2.29 (d, 2H, *J* = 7.1 Hz, C4-H); 2.22 – 1.71 (m, 12H); 2.01 (s, 3H, $COCH_3$) 1.71 – 1.37 (m, 14H); 1.37 – 0.79 (m, 16H); 0.62 (s, 3H, C18-H). ^{13}C NMR (75 MHz, $CDCl_3$) δ 170.5 (C=O); 143.2 (C, $C4_{triazole}$); 139.6 (C, C5); 132.6 (C, C=CH); 132.1 (C, C=CH); 123.4 (C, C=CH); 123.2 (CH, $C5_{triazole}$); 122.8 (CH, C6); 122.3 (CH, C=CH); 117.7 (CH, C=CH); 116.9 (CH, C=CH); 73.8 (CH, C3); 56.4 (CH); 56.0 (CH); 54.9 (CH); 49.8 (CH); 48.0 (CH_2); 47.8 (CH_2); 42.2 (C); 40.2 (CH_2); 39.4 (CH_2); 39.1 (CH_2); 38.0 (CH_2); 36.9 (CH_2); 36.5 (C); 32.1 (CH_2); 31.7 (CH); 31.6 (CH_2); 27.7 (CH_2); 27.1 (CH_2); 26.3 (CH_2); 26.2 (CH_2); 25.7 (CH_3); 24.2(CH_2); 23.4 (CH_3); 21.4 (CH_2); 20.8 (CH_2); 19.3 (CH_3); 17.7 (CH_3); 17.6 (CH_3); 16.5 (CH_3); 12.0 (CH_3). IR υ_{max} 3401 (N-H), 3045 (=C-H), 2899 (-C-H), 1750 (C=O), 1658 (-C=C-), 1444 cm^{-1}. HRMS calculated mass for $C_{36}H_{57}N_4O_2$ ($M+H^+$) 577.4476; found m/z 577.4475.

4.2.9.10. Synthesis of 20-(*S*)-((1-(3-phenylpropyl)-*1H*-1,2,3-triazol-4-yl)methyl)amino-5-pregnen-3β-ol acetate (D5)

Following the general reaction conditions for CuAAC reaction, the reaction was worked up and purified to afford 60 mg of a white solid (isolated yield: 85%). M.P.: 92.5 – 94.2 °C. Specific rotation [α] = -26.33 (c = 0.24 %, CH_2Cl_2). ^{1}H NMR (300 MHz, $CDCl_3$) δ 7.49 (s, 1H, $C5_{triazole}$-H); 7.37 – 7.24 (m, 2H, *m*-aromatic); 7.24 – 7.08 (m, 3H, *p*- and *o*-aromatic); 5.35 (d, 1H, *J* = 4.4 Hz, C6-H); 4.70 – 4.49 (m, 1H, C3-H); 4.32 (t, 2H, *J* = 7.1 Hz, $N1_{triazole}$-CH_2); 4.01 (d, 1H, *J* = 13.7 Hz, NH-CH_2); 3.81 (d, 1H, *J* = 13.7 Hz, NH-CH_2-); 2.63 (t, 2H, *J* = 7.5 Hz, CH_2-phenyl); 2.56 (m, 3H, C4-H, C20-H); 2.32 (m, 2H, C4-H); 2.22 (q, 2H, *J* = 7.2 Hz, $N1_{triazole}$-CH_2–CH_2–); 2.01 (s, 3H, $COCH_3$); 1.99-1.73 (m, 5H); 1.73 – 1.27 (m, 8H); 1.27 – 0.81 (m, 11H); 0.65 (s, 3H, C18-H). ^{13}C NMR (75 MHz, $CDCl_3$) δ 170.5 (C=O); 146.5 (C, $C4_{triazole}$); 140.2 (C, ipso-aromatic); 139.6 (C, C5); 128.6 (CH, *m*-aromatic); 128.4 (CH, *o*-aromatic); 126.3 (CH, *p*-aromatic); 122.5 (CH,

C6); 121.8 (CH, $C5_{triazole}$); 73.9 (CH, C3); 56.5 (CH); 56.1 (CH); 55.9 (CH); 49.9 (CH); 49.5 CH_2, CH_2-phenyl); 42.0 (CH_2, NH-CH_2-); 41.4 (C); 39.2 (CH_2); 38.1 (CH_2); 37.0 (CH_2); 36.6 (C); 32.5 ($N1_{triazole}$-CH_2); 31.8 (CH_2); 31.7 (CH_2); 27.7 (CH_2); 27.1 (CH_2); 24.1 (CH_2); 21.4 (CH_2); 20.9 (CH_2); 19.3 (CH_3); 18.8 (CH_2); 12.2 (CH_2). IR υ_{max} 3400 (N-H), 3015 (=C-H), 2920 (-C-H), 1732 (C=O), 1455 cm^{-1}. HRMS calculated mass for $C_{35}H_{51}N_4O_2$ ($M+H^+$) 559.4007; found m/z 559.4012.

4.2.9.11. Synthesis of 20-(*R*)-((1-benzyl-*1H*-1,2,3-triazol-4-yl)methyl)aminomethyl-5-pregnen-3β,20-diol (E1)

Following the general reaction conditions for CuAAC reaction, the reaction was worked up and purified to afford 53 mg of a light-yellow solid (isolated yield: 79%). M.P.: 244.6 – 246.3 °C (decomposition). Specific rotation [α] = -21.51 (c = 0.14 %, CH_2Cl_2). ^{1}H NMR (300 MHz, $CDCl_3$) δ 7.36 (m, 4H, $C4_{triazole}$-H, *m*- and *p*-aromatic); 7.27 (m, 2H, *o*-aromatic); 5.51 (s, 2H, CH_2-phenyl); 5.41 – 5.29 (m, 1H, C6-H); 3.92 (s, 2H, NH-CH_2-triazole); 3.63 – 3.38 (m, 1H, C3-H); 3.01 – 2.83 (m, 1H); 2.54 (s, 2H, C22-H); 2.43 – 1.91 (m, 12H); 1.83 (m, 3H); 1.73 – 1.31 (m, 11H); 1.23 (m, 7H); 1.03 – 0.61 (m, 10H). ^{13}C NMR (75 MHz, $CDCl_3$) δ 140.8 (C, C5); 134.7 (C, $C4_{triazole}$); 129.1 (C, ipso-aromatic); 129.1 (CH, m-aromatic); 128.8 (CH, p-aromatic); 128.0 (CH, o-aromatic); 121.6 (CH, C6); 121.6 (CH, $C5_{triazole}$); 73.1 (C, C20); 71.8 (CH, C3); 58.7 (CH_2, C22); 57.5 (CH); 56.9 (CH); 54.2 (CH_2, CH_2–phenyl); 52.3 (CH_2, NH-CH_2-triazole); 50.0 (CH); 42.7 (C); 42.3 (CH_2); 40.0 (CH_2); 37.2 (CH_2); 36.5 (C); 31.8 (CH); 31.4 (CH_2); 29.7 (CH_2); 25.6 (CH_2); 25.1 (CH_3, C21); 23.9 (CH_2); 22.4 (CH_2); 19.4 (CH_3, C19); 13.5 (CH_3, C18). IR υ_{max} 3433 (O-H), 3323 (N-H), 3020 (=C-H), 2923 (-C-H), 1456 cm^{-1}. HRMS calculated mass for $C_{32}H_{47}N_4O_2$ ($M+H^+$) 519.3694; found m/z 519.3688

4.2.9.12. Synthesis of 20-(*R*)-((1-(2-ethoxy-2-oxoethan-1-yl)-*1H*-1,2,3-triazol-4-yl)methyl)aminomethyl-5-pregnen-3β,20-diol (E2)

Following the general reaction conditions for CuAAC reaction, the reaction was worked up and purified to afford 60 mg of a light-yellow solid (isolated yield: 90%). M.P.: 175.3 – 177.4 °C. Specific rotation [α] = -26.38 (c = 0.11 %, CH_2Cl_2). ^{1}H NMR (300 MHz, $CDCl_3$) δ 7.60 (s, 1H, $C5_{triazole}$-H); 5.32 (s, 1H, C6-H); 5.11 (s, 2H, $N1_{triazole}$-CH_2); 4.24 (q, 2H, *J* = 7.1 Hz, C(O)OCH_2-); 3.94 (s, 2H, NH-

CH_2-triazole); 3.49 (m, 1H,C3-H); 2.68 – 2.33 (m, 6H); 2.23 (m, 3H); 2.14 – 1.86 (m, 4H); 1.79 (m, 3H); 1.45 (m, 10H); 1.25 (m, 12H); 0.89 (m, 12H). ^{13}C NMR (75 MHz, $CDCl_3$) δ 166.3 (C=O); 146.6 (C, C5); 140.8 (C, $C4_{triazole}$); 123.6 (CH, C6); 121.5 (CH, $C5_{triazole}$); 73.3 (C, C20); 71.7 (CH, C3); 62.4 (CH_2, O-CH_2); 58.7 (CH_2, C22); 56.6 (CH); 55.9 (CH); 50.9 ($N1_{triazole}$-CH_2); 50.0 (CH); 42.3 (CH_2); 42.0 (C); 41.1 (CH_2); 39.3 (CH_2); 37.2 (CH_2); 36.5 (C); 31.8 (CH_2); 31.7 (CH_2); 31.6 (CH); 27.1 (CH_2); 25.7 (CH_3); 24.2 (CH_2); 20.9 (CH_2); 19.4 (CH_3); 14.1 (CH_3, O-CH_2-CH_3); 13.2 (CH_3). IR υ_{max} 3446 (O-H), 3351 (N-H) 2924 (-C-H), 2851 (-C-H), 1749 (C=O), 1465 cm^{-1}. HRMS calculated mass for $C_{29}H_{47}N_4O_4$ ($M+H^+$) 515.3592; found m/z 515.3595.

4.2.9.13. Synthesis of 20-(*R*)-((1-octyl-*1H*-1,2,3-triazol-4-yl)methyl)aminomethyl-5-pregnen-3β,20-diol (E3)

Following the general reaction conditions for CuAAC reaction, the reaction was worked up and purified to afford 60 mg of a light-yellow solid (isolated yield: 85%). M.P.: 142.3 – 143.8 °C. Specific rotation [α] = -26.81 (c = 0.15 %, CH_2Cl_2).^{1}H NMR (300 MHz, $CDCl_3$) δ 7.58 (s, 1H, $C5_{triazole}$-H); 5.33 (d, 1H, *J* = 4.9 Hz, C6-H); 4.33 (t, 2H, *J* = 7.2 Hz, N1triazole-CH_2-); 4.04 (s, 2H, NH-CH_2-triazole); 3.50 (m, 1H, C3-H); 2.72 (d, 1H, *J* = 12.2 Hz, C22-H); 2.62 (d, 1H, *J* = 12.2 Hz, C22-H); 2.26 (m, 2H); 2.00 – 1.70 (m, 8H); 1.71 – 1.37 (m, 9H); 1.28 (m, 14H); 1.20 – 1.03 (m, 3H); 0.99 (m, 6H); 0.86 (m, 7H). ^{13}C NMR (75 MHz, $CDCl_3$) δ 144.1 (C, C5); 140.8 (C, $C4_{triazole}$); 122.5 (CH, C6); 121.5 (CH, $C5_{triazole}$); 73.0 (C, C20); 71.7 (CH, C3); 57.9 (CH); 57.7 (CH_2, C22); 56.9 (CH); 50.5 (CH_2, $N1_{triazole}$-CH_2); 50.0 (CH); 44.3 (CH_2); 42.7 (C); 42.2 (CH_2); 40.0 (CH_2); 37.2 (CH_2); 36.5 (C); 31.7 (CH); 31.6 (CH_2); 31.3 (CH_2); 30.3 (CH_2); 29.1 (CH_2); 29.0 (CH_2); 29.0 (CH_2); 26.5 (CH_2); 24.8 (CH_3); 23.8 (CH_2); 22.6 (CH_2); 22.4 (CH_2); 20.9 (CH_2); 19.4 (CH_3); 14.1 (CH_3, heptyl-CH_3); 13.5 (CH_2, C18). IR υ_{max} 3431 (O-H), 3388 (N-H), 2927 (-C-H), 2856 (-C-H), 1456 cm^{-1}. HRMS calculated mass for $C_{33}H_{57}N_4O_2$ ($M+H^+$) 541.4476; found m/z 541.4476.

4.2.9.14. Synthesis of 20-(*R*)-((1-(3,7-dimethylocta-2,6-dien-1-yl)-*1H*-1,2,3-triazol-4-yl)methyl)aminomethyl-5-pregnen-3β,20-diol (E4)

Following the general reaction conditions for CuAAC reaction, the reaction was worked up and purified to afford 59 mg of a white solid (isolated yield: 81%). M.P.: 72.0 – 73.8 °C. Specific rotation [α] = -25.87 (c = 0.14 %, CH_2Cl_2). ^{1}H NMR (300 MHz, $CDCl_3$) δ 7.49 (bs, 1H, $C5_{triazole}$-H); 5.40 (t, *J* = 7.4 Hz, 1H, CH=C); 5.32 (d, 1H, *J* = 3.9 Hz, C6-H); 5.14 – 4.99 (m, 1H, CH=C); 4.93 (t, 2H, *J* = 7.0 Hz, $N1_{triazole}$-CH_2); 3.98 (s, 2H, NH-CH_2-triazole); 3.50 (m, 3H, C3-H); 2.78 – 2.43 (m, 2H, C4-H); 2.37 – 1.89 (m, 10H); 1.78 (m, 6H); 1.73 – 1.31 (m, 16H); 1.24 (s, 7H); 1.02 – 0.70 (m, 9H). ^{13}C NMR (75 MHz, $CDCl_3$) δ 143.4 (C, $C4_{triazole}$); 143.2 (C, C=CH); 140.8 (C, C5); 132.1 (C, C=CH); 123.4 (CH, C=CH); 123.2 (CH, C=CH); 121.5 (CH, C6); 117.7 (CH, $C5_{triazole}$*Z*); 116.9 (CH, $C5_{triazole}$*E*); 71.7 (CH, C3); 58.2 (CH_2, C22); 57.7 (CH); 56.9 (CH); 50.0 (CH); 48.0 ($N1_{triazole}$-CH_2); 44.6 (CH_2); 42.7 (CH_2); 42.2 (C); 40.0 (CH_2); 39.4 (CH_2); 37.2 (CH_2); 36.5 (C); 32.1 (CH_2); 31.8 (CH); 31.6 (CH_2); 31.4 (CH_2); 26.3 (CH_2); 26.1; 25.7 (CH_3); 25.5 (CH_3); 24.9 (CH_3); 23.9 (CH_2); 23.4 (CH_2); 22.4 (CH_2); 20.9 (CH_2); 19.4 (CH_3); 17.7 (CH_3); 16.5 (CH_3); 13.5 (CH_3). IR υ_{max} 3300 (O-H), 2998 (=C-H), 2884 (-C-H), 1646, 1444 cm^{-1}. HRMS calculated mass for $C_{35}H_{57}N_4O_2$ ($M+H^+$) 565.4476; found m/z 565.4477.

4.2.9.15. Synthesis of 20-(*R*)-((1-(3-phenylpropyl)-*1H*-1,2,3-triazol-4-yl)methyl)aminomethyl-5-pregnen-3β,20-diol (E5)

Following the general reaction conditions for CuAAC reaction, the reaction was worked up and purified to afford 50 mg of a light-yellow solid (isolated yield: 71%). M.P.: 191.9 – 192.5 °C (decomposition). Specific rotation [α] = -20.83 (c = 0.12 %, CH_2Cl_2). ^{1}H NMR (300 MHz, $CDCl_3$) δ 7.46 (s, 1H, $C5_{triazole}$-H); 7.36 – 7.08 (m, 5H, aromatics); 5.34 (d, 1H, *J* = 5.0 Hz, C6-H); 4.34 (t, 2H, *J* = 7.1 Hz, $N1_{triazole}$-CH_2); 3.95 (s, 2H, NH-CH_2-triazole); 3.50 (d, 1H, *J* = 5.6 Hz, C6-H); 3.28 (m, 1H); 2.65 (t, 2H, *J* = 7.5 Hz, CH_2-phenyl); 2.57 (m, 2H); 2.41 – 2.14 (m, 5H); 1.96 (s, 7H); 1.89 – 1.73 (m, 4H); 1.73 – 1.31 (m, 10H); 1.23 (s, 4H); 1.13 (m, 5H); 0.99 (s, 6H); 0.83 (s, 4H). ^{13}C NMR (75 MHz, $CDCl_3$) δ 146.7 (C, $C4_{triazole}$); 140.9 (C, C5); 140.2 (C, ipso-aromatic); 128.6 (CH, *m*-aromatic); 128.4 (CH, *o*-aromatic); 126.3 (CH, p-aromatic); 121.7 (CH, C6); 121.4 (CH, $C5_{triazole}$); 73.3 (C, C20); 71.6 (CH, C3); 56.4 (CH); 56.0 (CH); 50.0 (CH_2); 49.5 (CH_2, CH_2-phenyl); 42.3 (CH_2); 42.1 (C); 41.6 (CH_2); 40.0 (CH_2); 37.2 (CH_2); 36.5 (C); 32.5 (CH_2, $N1_{triazole}$-CH_2); 31.8 (CH_2); 31.8 (CH_2); 31.7 (CH_2); 26.7 (CH_2); 25.5 (CH_3); 24.1 (CH_2);

21.1 (CH_2); 19.4 (CH_3); 18.8 (CH_3); 13.7 (CH_2). IR υ_{max} 3452 (O-H), 3314 (N-H) 2862 (-C-H), 1451 cm^{-1}. HRMS calculated mass for $C_{34}H_{51}N_4O_2$ ($M+H^+$) 547.4007; found m/z 547.4007.

4.2.9.16. Synthesis of 20-(*R*)-(4-phenyl-*1H*-1,2,3-triazol-1-yl)methyl-5-pregnen-3β,20-diol (F1)

Following the general reaction conditions for CuAAC reaction, the reaction was worked up and purified to afford 46 mg of a white solid (isolated yield: 69%). M.P.: 208.5 – 210.0 °C (decomposition). Specific rotation [α] = -42.14 (c = 0.14 %, CH_2Cl_2). ^{1}H NMR (300 MHz, $CDCl_3$) δ 7.90 (s, 1H, $C5_{triazole}$-H); 7.85 (d, 2H, *J* = 7.7 Hz, *o*-aromatic); 7.43 (t, 2H, *J* = 7.5 Hz, *m*-aromatic); 7.33 (t, 1H, *J* = 7.4 Hz, *p*-aromatic); 5.36 (d, 1H, *J* = 5.1 Hz, C6-H); 4.34 (d, 2H, *J* = 4.6 Hz, C22-H); 3.52 (m, 1H, C3-H); 2.29 (m, 2H, C4-H); 2.18 – 1.65 (m, 9H); 1.65 – 1.38 (m, 10H); 1.22 (m, 6H); 0.97 (m, 9H). ^{13}C NMR (75 MHz, $CDCl_3$) δ 147.4 (C, $C4_{triazole}$); 140.8 (C, C5); 130.3 (C, ipso-aromatic); 128.8 (CH, *m*-aromatic); 128.2 (CH, *o*-aromatic); 125.5 (CH, *p*-aromatic); 122.0 (CH, $C4_{triazole}$); 121.3 (CH, C6); 74.2 (C, C20); 71.1 (CH, C3); 60.2 (CH_2, C22); 57.5 (CH); 56.7 (CH); 49.9 (CH); 43.0 (C); 41.7 (CH_2); 40.0 (CH_2); 37.2 (CH_2); 36.4 (C); 31.6 (CH_2); 31.6 (CH_2); 31.3 (CH_2); 23.8 (CH_2); 23.4 (CH_3, C21); 22.2 (CH_2); 20.8 (CH_2); 19.1 (CH_3, C19); 13.2 (CH_3, C18). IR υ_{max} 3489 (O-H), 3050 (=C-H), 2933 (-C-H), 1457 cm^{-1}. HRMS calculated mass for $C_{30}H_{41}N_3O_2Na$ ($M+Na^+$) 498.3091; found m/z 498.3068.

4.2.9.17. Synthesis of 20-(*R*)-(4-(1-methoxy-1-oxomethyl)-*1H*-1,2,3-triazol-1-yl)methyl-5-pregnen-3β,20-diol (F2)

Following the general reaction conditions for CuAAC reaction, the reaction was worked up and purified to afford 47 mg of a white solid (isolated yield: 73%). M.P.: 179.7 – 181.5 °C. Specific rotation [α] = -42.56 (c = 0.13 %, CH_2Cl_2). ^{1}H NMR (300 MHz, $CDCl_3$) δ 8.24 (s, 1H, $C5_{triazole}$-H); 5.36 (d, 1H, *J* = 5.1 Hz, C6-H); 4.49 – 4.17 (m, 2H, C22-H); 3.95 (s, 3H, O-CH_3); 3.53 (s, 1H, C3-H); 2.29 (m, 2H, C4-H); 2.16 – 1.63 (m, 9H); 1.63 – 1.37 (m, 13H); 1.25 (s, 3H); 1.18 – 0.71 (m, 12H). ^{13}C NMR (75 MHz, $CDCl_3$) δ 161.3 (C=O), 140.8 (C, C5), 139.7 (C=O), 129.3 (C, $C4_{triazole}$), 121.4 ($C5_{triazole}$), 74.7 (C, C20), 71.7 (CH, C3), 59.9 (CH_3, O-CH_3), 57.4 (CH), 56.6 (CH), 52.2 (CH_2), 49.9 (CH), 43.2 (C), 42.2 (CH_2), 40.0 (CH_2), 37.2 (CH_2), 36.5 (C), 31.7 (CH_2), 31.6 (CH_2), 31.3 (CH), 24.5 (CH_3, C21), 23.9 (CH_2), 22.3 (CH_2), 20.8 (CH_2), 19.4 (CH_3,

C19), 13.6 (CH_3, C18). IR υ_{max} 3468 (O-H), 3048 (=C-H), 2933 (-C-H); 1740 (C=O); 1476 cm^{-1}. HRMS calculated mass for $C_{26}H_{39}N_3O_4Na$ ($M+Na^+$) 480.2833; found m/z 480.2821.

4.2.9.18. Synthesis of 20-(*R*)-(4-pentyl-*1H*-1,2,3-triazol-1-yl)methyl-5-pregnen-3β,20-diol (F3)

Following the general reaction conditions for CuAAC reaction, the reaction was worked up and purified to afford 54 mg of a white solid (isolated yield: 86%). M.P.: 141.1 – 142.9 °C. Specific rotation [α] = -33.38 (c = 0.13 %, CH_2Cl_2). ^1H NMR (300 MHz, $CDCl_3$) δ 7.37 (s, 1H, $C5_{triazole}$-H); 5.33 (d, 1H, *J* = 5.0 Hz, C6-H); 4.23 (s, 2H, C22-H); 3.51 (dt, 1H, *J* = 11.3, 6.0 Hz, C3); 2.69 (t, 2H, *J* = 7.7 Hz, $C4_{triazole}$-CH_2-); 2.36 – 2.04 (m, 4H); 2.04 – 1.74 (m, 7H); 1.68 (p, *J* = 7.9 Hz, 4H); 1.50 (d, *J* = 5.5 Hz, 6H); 1.40 – 1.16 (m, 6H); 1.16 – 0.77 (m, 16H). ^{13}C NMR (75 MHz, $CDCl_3$) δ 148.1 (C, $C4_{triazole}$); 140.8 (C, C5); 122.5 (CH, $C5_{triazole}$); 121.4 (CH, C6); 74.7 (C, C20); 71.6 (CH, C3); 59.8 (CH_2, C22); 57.4 (CH); 56.7 (CH); 49.9 (CH); 43.2 (C); 42.2 (CH_2); 40.0 (CH_2); 37.2 (CH_2); 36.5 (C); 31.7 (CH_2); 31.6 (CH_2); 31.4 (CH_2); 31.3 (CH_2); 29.1 (CH_2); 25.6 (CH_2); 24.5 (CH_3, C21); 23.9 (CH_2); 22.4 (CH_2); 22.3 (CH_2); 20.9 (CH_2); 19.4 (CH_3, C19); 14.0 (CH_3, heptyl-CH_3); 13.5 (CH_3, C18). IR υ_{max} 3447 (O-H), 3058 (=C-H), 2932 (-C-H), 1486 cm^{-1}. HRMS calculated mass for $C_{29}H_{48}N_3O_2$ ($M+H^+$) 470.3741; found m/z 470.3736.

4.2.9.19. Synthesis of 20-(*R*)-(4-(2-hydroxyethyl)-*1H*-1,2,3-triazol-1-yl)methyl-5-pregnen-3β,20-diol (F4)

Following the general reaction conditions for CuAAC reaction, the reaction was worked up and purified to afford 61 mg of a white solid (isolated yield: 97%). M.P.: 169.6 – 171.7 °C. Specific rotation [α] = -43.24 (c = 0.22 %, CH_2Cl_2). ^1H NMR (300 MHz, $CDCl_3$) δ 7.50 (s, 1H, $C5_{triazole}$-H); 5.35 (d, 1H, *J* = 5.3 Hz, C6-H); 4.27 (s, 2H, C22-H); 3.96 (t, 2H, *J* = 5.8 Hz, CH_2-OH); 3.54 (m, 1H, C3-H); 2.96 (t, 2H, *J* = 5.8 Hz, $C4_{triazole}$-CH_2); 2.47 – 2.00 (m, 6H); 1.84 (m, 10H); 1.52 (m, 15H); 1.07 (m, 13H); 0.90 (s, 3H, C18-H). ^{13}C NMR (75 MHz, $CDCl_3$) δ 140.8 ppm (C, $C4_{triazole}$); 140.8 (C, C5); 123.5 (CH, $CH_{triazole}$); 121.5 (CH, C6); 74.7 (C, C20); 71.7 (CH, C3); 61.7 (CH_2, CH_2-OH); 59.8 (CH_2, C22); 57.3 (CH); 56.7 (CH); 49.9 (CH); 43.2 (C); 42.2 (CH_2); 40.0 (CH_2); 37.2 (CH_2); 36.5 (C); 31.7 (CH_2); 31.6 (CH_2); 31.3 (CH_2); 28.6 (CH_2, $C4_{triazole}$-CH_2) 24.5 (CH_3, C21); 23.9 (CH_2); 22.3 (CH_2); 20.9 (CH_2); 19.4 (CH_3, C19); 13.6 (CH_3, C18). IR

υ_{max} 3421 (O-H), 3028 (=C-H), 2932 (-C-H), 1454 cm^{-1}. HRMS calculated mass for $C_{26}H_{41}N_3O_3Na$ ($M+Na^+$) 466.3040; found m/z 466.2996.

4.2.9.20. Synthesis of 20-(*R*)-(4-(3-phenylpropyl)-*1H*-1,2,3-triazol-1-yl)methyl-5-pregnen-3β,20-diol (F5)

Following the general procedure for CuAAC reaction, the reaction was worked up and purified to afford 67 mg of a white solid (isolated yield: 92%). M.P.: 187.4 – 189.5 °C (decomposition). Specific rotation [α] = -57.94 (c = 0.14 %, CH_2Cl_2). ^{1}H NMR (300 MHz, $CDCl_3$) δ 7.37 (s, 1H, C5triazole-H); 7.32 – 7.22 (m, 2H, *m*-aromatic); 7.17 (m, 3H, *o*- and *p*-aromatic); 5.34 (d, 1H, *J* = 5.0 Hz, C6-H); 4.23 (s, 2H, NH-CH_2-triazol); 3.51 (dt, 1H, *J* = 11.5, 6.0 Hz, C3-H); 2.74 (t, 2H, *J* = 7.7 Hz, $N1_{triazole}$-CH_2); 2.67 (t, 2H, *J* = 7.7 Hz, CH_2-phenyl); 2.35 – 2.17 (m, 2H, C4-H); 2.03 (m, 6H); 1.89 – 1.60 (m, 7H); 1.50 (s, 6H); 1.25 (m, 3H); 1.11 (s, 3H); 1.00 (m, 6H); 0.88 (s, 3H, C18-H). ^{13}C NMR (75 MHz, $CDCl_3$) δ 147.5 (C, $C4_{triazole}$); 141.9 (C, ipso-aromatic), 140.8 (C, C5); 128.5 (CH, *m*-aromatic); 128.3 (CH, *o*-aromatic) 125.8 (CH , *p*-aromatic); 122.7 (CH, $C5_{triazole}$); 121.4 (CH, C6); 74.7 (C, C20); 71.6 (CH, C3); 59.8 (CH_2, C22); 57.3 (CH); 56.8 (CH); 49.9 (CH); 43.2 (C); 42.2 (CH_2); 40.0 (CH_2); 37.2 (CH_2); 36.5 (C); 35.3 (CH_2); 31.7 (CH_2); 31.6 (CH_2); 31.3 (CH_2); 31.1 (CH_2); 25.2 (CH_2); 24.5 (CH_3, C21); 23.9 (CH_2); 22.3 (CH_2); 20.9 (CH_2); 19.4 (CH_3, C19);13.2 (CH_3, C18). IR υ_{max} 3347 (O-H), 3040 (=C-H), 2922 (-C-H), 1458 cm^{-1}. HRMS calculated mass for $C_{33}H_{47}N_3O_2Na$ ($M+Na^+$) 540.3561; found m/z 540.3533.

4.3. *In vitro* activity against *L. donovani* (IC_{50})

Antileishmanial activity of the compounds was tested in vitro on a culture of *Leishmania donovani* promastigotes (strain S1). Compounds with appropriate dilution were added to a 96 well microplate with promastigotes ($2x10^6$ cell/mL) reaching final concentrations in the range of 1.6 to 40 µg/mL. The plates were incubated at 26°C for 72 h and growth was determined by Alamar blue assay [51]. Pentamidine and amphotericin B were tested as the standard antileishmanial agents and DMSO was used as negative control. IC_{50} values were calculated by dose-response analysis with XL-Fit®

4.4. *In vitro* activity against *T. brucei* (IC_{50})

T. brucei BSF parasites were seeded at 1 x 10^3 parasites/ml in 200 µL growth medium containing different concentrations of triazolylsterols. After incubation at 37ºC for 3 days, 20 µL Alamar blue (Biosource UK Ltd) was added to each well and the plates incubated for a further 16 hours. The fluorescence of each culture was determined as described above and the IC_{50} value for each compound were determined from the dose response curves. The standard agent Nifurtimox was used as the positive control and DMSO as negative control.

4.5. *In vitro* activity against *T. cruzi* (IC_{50})

T. cruzi epimastigotes were seeded at 5x10^5 parasites/ml in 200 µL growth medium containing different concentrations of triazolylsterols and 20 µL Alamar blue™ (Biosource UK Ltd) was added to each well. After incubation at 27 ºC for 14 days, the cell densities were determined by monitoring the fluorescence of each culture using a Gemini Fluorescent Plate reader (Molecular Devices) at an excitation wavelength of 530 nm, emission wavelength of 585 nm and a filter cut off at 550 nm, and the IC_{50} values were determined. The colour change resulting from the reduction of Alamar blue is proportional to the number of live cells, which was established following production of a standard curve. The standard anti-Chagas agent Nifurtimox was used as the positive control and DMSO as negative control.

4.6. Vero Cell activities

The *in vitro* cytotoxicity was determined against mammalian kidney fibroblasts (VERO). The assay was performed in 96-well tissue culture-treated plates as described earlier. Briefly, cells were seeded to the wells of the plate (25,000 cells/well) and incubated for 24 h. Samples were added, and plates were again incubated for 48 h. The number of viable cells was counted and the plot for EC_{50} performed.

4.7. Physicochemical properties prediction

SMILES of compounds **A1** – **F5** were pasted on the Osiris DataWarrior platform [52], and relevant properties were predicted (Total Molweight, cLogP, cLogS, H-Acceptors, H-Donors, Total Surface Area, Relative PSA, Polar Surface Area, Druglikeness, Mutagenic, Tumorigenic, Reproductive Effective, Irritant). $LogD_{7.4}$ was also predicted, using the online ChemAxon LogD predictor [46].

4.8. ADMETox predictions

Computational modelling to estimate the bioavailability, aqueous solubility, human intestinal absorption, metabolism, mutagenicity, toxicity, etc. for the compounds was performed using the SwissADME [44] and pkCSM [53] platforms.

SwissADME: The SMILES of compounds **A1** – **F5** were uploaded to SwissADME (http://www.swissadme.ch/), pasting the list of smiles on the designated window. The following parameters were calculated: *Physicochemical Properties* (Formula, MW, Num. heavy atoms, Num. arom. heavy atoms, Fraction Csp3, Num. rotatable bonds, Num. H-bond acceptors, Num. H-bond donors, Molar Refractivity and TPSA); *Lipophilicity* (Log Po/w (iLOGP), Log Po/w (XLOGP3), Log Po/w (WLOGP), Log Po/w (MLOGP), Log Po/w (SILICOS-IT) and Consensus Log Po/w); *Water Solubility* (Log S (ESOL), Solubility, Class, Log S (Ali), Solubility, Class, Log S (SILICOS-IT), Solubility and Class); *Pharmacokinetics* (GI absorption, BBB permeant, P-gp substrate, CYP1A2 inhibitor, CYP2C19 inhibitor, CYP2C9 inhibitor, CYP2D6 inhibitor, CYP3A4 inhibitor and Log Kp -skin permeation-); *Druglikeness* (Lipinski, Ghose, Veber, Egan, Muegge and Bioavailability Score); *Medicinal Chemistry* (PAINS, Brenk, Lead likeness and Synthetic accessibility).

pkCSM: The SMILES of compounds **A1** – **F5** were uploaded to pkCSM (http://biosig.unimelb.edu.au/pkcsm/prediction), through a *.txt SMILE file. The following parameters were calculated: *Absorption* (Water solubility, Caco2 permeability, Intestinal absorption (human), Skin Permeability, P-glycoprotein substrate, P-glycoprotein I inhibitor, P-glycoprotein II inhibitor); *Distribution* (VDss (human), Fraction unbound (human), BBB permeability, CNS permeability); *Metabolism* (CYP2D6 substrate, CYP3A4 substrate, CYP1A2 inhibitor, CYP2C19 inhibitor, CYP2C9 inhibitor, CYP2D6 inhibitor, CYP3A4 inhibitor); *Excretion* (Total Clearance, Renal OCT2 substrate); *Toxicity* (AMES toxicity, Max. tolerated dose (human), hERG I inhibitor, hERG II inhibitor, Oral Rat Acute Toxicity (LD_{50}), Oral Rat Chronic Toxicity (LOAEL), Hepatotoxicity, Skin Sensitization, *T. pyriformis* toxicity, Minnow toxicity).

Acknowledgements

This work was supported in part by grants from the National Research Council of Argentina, CONICET (CONICET (PIP 2021-2023 11220200101045CO to G.R.L.); Agencia Nacional de Promoción Científica y Tecnológica, ANPCyT-Argentina (ANPCyT PICT- 2017-2096

awarded to G.R.L.); UNR (Universidad Nacional de Rosario 80020190300101UR) and Fundación Josefina Prats. The research leading to these results has, in part, received funding from the UK Research and Innovation via the Global Challenges Research Fund under grant agreement A Global Network for Neglected Tropical Diseases grant number MR/P027989/1. G.R.L. is a member of the scientific staff of CONICET-Argentina. E.O.J.P., M.S.B. and R.C. thank CONICET for the award of a fellowship.

References

[1] World Health Organization, (n.d.). http://www.who.int.

[2] V. Pillay-van Wyk, D. Bradshaw, Mortality and socioeconomic status: the vicious cycle between poverty and ill health, Lancet Glob Health. 5 (2017) e851–e852. https://doi.org/10.1016/S2214-109X(17)30304-2.

[3] D.H. Molyneux, L. Savioli, D. Engels, Neglected tropical diseases: progress towards addressing the chronic pandemic, The Lancet. 389 (2017) 312–325. https://doi.org/10.1016/S0140-6736(16)30171-4.

[4] R.G.A. Feachem, I. Chen, O. Akbari, A. Bertozzi-Villa, S. Bhatt, F. Binka, M.F. Boni, C. Buckee, J. Dieleman, A. Dondorp, A. Eapen, N. Sekhri Feachem, S. Filler, P. Gething, R. Gosling, A. Haakenstad, K. Harvard, A. Hatefi, D. Jamison, K.E. Jones, C. Karema, R.N. Kamwi, A. Lal, E. Larson, M. Lees, N.F. Lobo, A.E. Micah, B. Moonen, G. Newby, X. Ning, M. Pate, M. Quiñones, M. Roh, B. Rolfe, D. Shanks, B. Singh, K. Staley, J. Tulloch, J. Wegbreit, H.J. Woo, W. Mpanju-Shumbusho, Malaria eradication within a generation: ambitious, achievable, and necessary, The Lancet. 394 (2019) 1056–1112. https://doi.org/10.1016/S0140-6736(19)31139-0.

[5] S. Warusavithana, H. Atta, M. Osman, Y. Hutin, Review of the neglected tropical diseases programme implementation during 2012–2019 in the WHO-Eastern Mediterranean Region, PLoS Negl Trop Dis. 16 (2022) e0010665. https://doi.org/10.1371/journal.pntd.0010665.

[6] L. Urán Landaburu, M. Didier Garnham, F. Agüero, Targeting trypanosomes: how chemogenomics and artificial intelligence can guide drug discovery, Biochem Soc Trans. 51 (2023) 195–206. https://doi.org/10.1042/BST20220618.

[7] D. Horn, A profile of research on the parasitic trypanosomatids and the diseases they cause, PLoS Negl Trop Dis. 16 (2022). https://doi.org/10.1371/journal.pntd.0010040.

[8] S. Aksoy, P. Buscher, M. Lehane, P. Solano, J. Van Den Abbeele, Human African trypanosomiasis control: Achievements and challenges, PLoS Negl Trop Dis. 11 (2017) e0005454. https://doi.org/10.1371/journal.pntd.0005454.

[9] W. Zhang, P. Lypaczewski, G. Matlashewski, Optimized CRISPR-Cas9 Genome Editing for Leishmania and Its Use To Target a Multigene Family, Induce Chromosomal Translocation, and Study DNA Break Repair Mechanisms, MSphere. 2 (2017) e00340-16. https://doi.org/10.1128/mSphere.00340-16.

[10] J. Jannin, P. Solano, I. Quick, P. Debre, The francophone network on neglected tropical diseases, PLoS Negl Trop Dis. 11 (2017) e0005738. https://doi.org/10.1371/journal.pntd.0005738.

[11] T. Beneke, R. Madden, L. Makin, J. Valli, J. Sunter, E. Gluenz, A CRISPR Cas9 high-throughput genome editing toolkit for kinetoplastids, R Soc Open Sci. 4 (2017) 170095. https://doi.org/10.1098/rsos.170095.

[12] A.J. Saviola, F. Negrão, J.R. Yates III, Proteomics of Select Neglected Tropical Diseases, Annual Review of Analytical Chemistry. 13 (2020) 315–336. https://doi.org/10.1146/annurev-anchem-091619-093003.

[13] S.T. de Macedo-Silva, W. de Souza, J.C.F. Rodrigues, Sterol biosynthesis pathway as an alternative for the anti-protozoan parasite chemotherapy, Curr Med Chem. 22 (2015) 2186–2198. https://doi.org/10.2174/0929867322666150319120337.

[14] J.A. Urbina, Lipid biosynthesis pathways as chemotherapeutic targets in kinetoplastid parasites, Parasitology. 114 (1997) S91–S99. https://doi.org/10.1017/S0031182097001194.

[15] J.F. Osorio-Méndez, A.M. Cevallos, Discovery and genetic validation of chemotherapeutic targets for Chagas' disease, Front Cell Infect Microbiol. 8 (2019) 439. https://doi.org/10.3389/fcimb.2018.00439.

[16] D.J. Leaver, Synthesis and biological activity of Sterol 14α-demethylase and Sterol C24-methyltransferase inhibitors, Molecules. 23 (2018). https://doi.org/10.3390/molecules23071753.

[17] W. Zhou, G.I. Lepesheva, M.R. Waterman, W.D. Nes, Mechanistic analysis of a multiple product sterol methyltransferase implicated in ergosterol biosynthesis in Trypanosoma brucei, Journal of Biological Chemistry. 281 (2006) 6290–6296. https://doi.org/10.1074/jbc.M511749200.

[18] L. Urán Landaburu, A.J. Berenstein, S. Videla, P. Maru, D. Shanmugam, A. Chernomoretz, F. Agüero, TDR Targets 6: Driving drug discovery for human pathogens through intensive chemogenomic data integration, Nucleic Acids Res. 48 (2020) D992–D1005. https://doi.org/10.1093/nar/gkz999.

[19] S. Mukherjee, W. Xu, F.F. Hsu, J. Patel, J. Huang, K. Zhang, Sterol methyltransferase is required for optimal mitochondrial function and virulence in Leishmania major, Mol Microbiol. 111 (2019) 65–81. https://doi.org/10.1111/mmi.14139.

[20] F. Gigante, M. Kaiser, R. Brun, I.H. Gilbert, SAR studies on azasterols as potential anti-trypanosomal and anti-leishmanial agents, Bioorg Med Chem. 17 (2009) 5950–5961. https://doi.org/10.1016/j.bmc.2009.06.062.

[21] L. Gros, S.O. Lorente, C. Jimenez, V. Yardley, L. Rattray, H. Wharton, S. Little, S.L. Croft, L.M. Ruiz-Perez, D. Gonzalez-Pacanowska, I.H. Gilbert, Evaluation of azasterols as anti-parasitics, J Med Chem. 49 (2006) 6094–6103. https://doi.org/10.1021/jm060290f.

[22] F. Magaraci, C. Jimenez Jimenez, C. Rodrigues, J.C.F. Rodrigues, M. Vianna Braga, V. Yardley, K. De Luca-Fradley, S.L. Croft, W. De Souza, L.M. Ruiz-Perez, J. Urbina, D. Gonzalez Pacanowska, I.H. Gilbert, Azasterols as Inhibitors of Sterol 24-Methyltransferase in

Leishmania Species and Trypanosoma cruzi, J Med Chem. 46 (2003) 4714–4727. https://doi.org/10.1021/jm021114j.

[23] E.O.J. Porta, P.B. Carvalho, M.A. Avery, B.L. Tekwani, G.R. Labadie, Click chemistry decoration of amino sterols as promising strategy to developed new leishmanicidal drugs, Steroids. 79 (2014) 28–36. https://doi.org/10.1016/j.steroids.2013.10.010.

[24] W.D. Nes, Sterol methyl transferase: enzymology and inhibition, Biochim Biophys Acta. 1529 (2000) 63–88. https://doi.org/10.1016/s1388-1981(00)00138-4.

[25] W.D. Nes, Enzyme redesign and interactions of substrate analogues with sterol methyltransferase to understand phytosterol diversity, reaction mechanism and the nature of the active site, Biochem Soc Trans. 33 (2005) 1189–1196. https://doi.org/10.1042/BST20051189.

[26] C. Jiménez-Jiménez, J. Carrero-Lérida, M. Sealey-Cardona, L.M. Ruiz Pérez, J.A. Urbina, D. González Pacanowska, Δ24(25)-sterol methenyltransferase: Intracellular localization and azasterol sensitivity in Leishmania major promastigotes overexpressing the enzyme, Mol Biochem Parasitol. 160 (2008) 52–59. https://doi.org/10.1016/j.molbiopara.2008.03.010.

[27] C. Jiménez-Jiménez, J. Carrero-Lérida, M. Sealey-Cardona, L.M. Ruiz Pérez, J.A. Urbina, D. González Pacanowska, Δ24(25)-sterol methenyltransferase: Intracellular localization and azasterol sensitivity in Leishmania major promastigotes overexpressing the enzyme, Mol Biochem Parasitol. 160 (2008) 52–59. https://doi.org/10.1016/j.molbiopara.2008.03.010.

[28] E.O.J. Porta, M.M. Vallejos, A.B.J. Bracca, G.R. Labadie, Experimental and theoretical studies of the [3,3]-sigmatropic rearrangement of prenyl azides, RSC Adv. 7 (2017) 47527–47538. https://doi.org/10.1039/c7ra09759j.

[29] M.M. Vallejos, G.R. Labadie, Insight into the factors controlling the equilibrium of allylic azides, RSC Adv. 10 (2020) 4404–4413. https://doi.org/10.1039/c9ra10093h.

[30] E.O.J. Porta, S.N. Jäger, I. Nocito, G.I. Lepesheva, E.C. Serra, B.L. Tekwani, G.R. Labadie, Antitrypanosomal and antileishmanial activity of prenyl-1,2,3-triazoles, Medchemcomm. 8 (2017) 1015–1021. https://doi.org/10.1039/c7md00008a.

[31] E.O.J. Porta, I. Bofill Verdaguer, C. Perez, C. Banchio, M. Ferreira De Azevedo, A.M. Katzin, G.R. Labadie, Repositioning Salirasib as a new antimalarial agent, Medchemcomm. 10 (2019) 1599–1605. https://doi.org/10.1039/c9md00298g.

[32] D.T. Fox, C.D. Poulter, Synthesis and evaluation of 1-deoxy-D-xylulose 5-phosphoric acid analogues as alternate substrates for methylerythritol phosphate synthase, Journal of Organic Chemistry. 70 (2005) 1978–1985. https://doi.org/10.1021/jo048022h.

[33] J.S. Li, Y. Li, C. Son, A.M.H. Brodie, Synthesis and evaluation of pregnane derivatives as inhibitors of human testicular 17α-hydroxylase/C17,20-lyase, J Med Chem. 39 (1996) 4335–4339. https://doi.org/10.1021/jm960245f.

[34] Y. Takeuchi, Y. Makino, K. Maruyama, E. Yoshii, A new 2-pyrone synthesis and its application to butadienolide synthesis, Heterocycles. 14 (1980) 163–168. https://doi.org/10.3987/R-1980-02-0163.

[35] J.S. Li, Y. Li, C. Son, A.M.H. Brodie, Synthesis and evaluation of pregnane derivatives as inhibitors of human testicular 17α-hydroxylase/C17,20-lyase, J Med Chem. 39 (1996) 4335–4339. https://doi.org/10.1021/jm960245f.

[36] M. Egido-Gabás, P. Serrano, J. Casas, A. Llebaria, A. Delgado, New aminocyclitols as modulators of glucosylceramide metabolism, Org Biomol Chem. 3 (2005) 1195–1201. https://doi.org/10.1039/b411473f.

[37] B. Colín-Lozano, I. León-Rivera, M.J. Chan-Bacab, B.O. Ortega-Morales, R. Moo-Puc, V. López-Guerrero, E. Hernández-Núñez, R. Argüello-Garcia, T. Scior, E. Barbosa-Cabrera, G. Navarrete-Vázquez, Synthesis, in vitro and in vivo giardicidal activity of nitrothiazole-NSAID chimeras displaying broad antiprotozoal spectrum, Bioorg Med Chem Lett. 27 (2017) 3490–3494. https://doi.org/10.1016/j.bmcl.2017.05.071.

[38] S. Bolden, C.A. Boateng, X.Y. Zhu, J.R. Etukala, S.K. Eyunni, M.R. Jacob, S.I. Khan, S.Y. Ablordeppey, CoMFA studies and in vitro evaluation of some 3-substituted benzylthio quinolinium salts as anticryptococcal agents, Bioorg Med Chem. 21 (2013) 7194–7201. https://doi.org/10.1016/j.bmc.2013.08.043.

[39] S. Girault, P. Grellier, A. Berecibar, L. Maes, E. Mouray, P. Lemière, M.A. Debreu, E. Davioud-Charvet, C. Sergheraert, Antimalarial, antitrypanosomal, and antileishmanial activities and cytotoxicity of bis(9-amino-6-chloro-2- methoxyacridines): Influence of the linker, J Med Chem. 43 (2000) 2646–2654. https://doi.org/10.1021/jm990946n.

[40] K. Katsuno, J.N. Burrows, K. Duncan, R.H. van Huijsduijnen, T. Kaneko, K. Kita, C.E. Mowbray, D. Schmatz, P. Warner, B.T. Slingsby, Hit and lead criteria in drug discovery for infectious diseases of the developing world, Nat Rev Drug Discov. 14 (2015) 751–8. https://doi.org/10.1038/nrd4683.

[41] J. Martín-Escolano, E. Medina-Carmona, R. Martín-Escolano, Chagas Disease: Current View of an Ancient and Global Chemotherapy Challenge, ACS Infect Dis. 6 (2020) 2830–2843. https://doi.org/10.1021/acsinfecdis.0c00353.

[42] T. Sander, J. Freyss, M. Von Korff, C. Rufener, DataWarrior: An open-source program for chemistry aware data visualization and analysis, J Chem Inf Model. 55 (2015) 460–473. https://doi.org/10.1021/ci500588j.

[43] ChemAxon Calculator and Predictors, (n.d.). https://chemaxon.com/ products/calculators-and-predictors.

[44] A. Daina, O. Michielin, V. Zoete, SwissADME: A free web tool to evaluate pharmacokinetics, drug-likeness and medicinal chemistry friendliness of small molecules, Sci Rep. 7 (2017) 42717. https://doi.org/10.1038/srep42717.

[45] D.E.V. Pires, T.L. Blundell, D.B. Ascher, pkCSM: Predicting small-molecule pharmacokinetic and toxicity properties using graph-based signatures, J Med Chem. 58 (2015) 4066–4072. https://doi.org/10.1021/acs.jmedchem.5b00104.

[46] ChemAxon Calculator and Predictors, (n.d.).

[47] L. Di, H. Rong, B. Feng, Demystifying Brain Penetration in Central Nervous System Drug Discovery, J Med Chem. 56 (2013) 2–12. https://doi.org/10.1021/jm301297f.

[48] Z. Szendi, P. Forgó, F. Sweet, Complete1H and 13C NMR spectra of pregnenolone, Steroids. 60 (1995) 442–446. https://doi.org/10.1016/0039-128x(94)00047-g.

[49] Z. Lin, S.R. Marepally, D. Ma, T.K. Kim, A.S. Oak, L.K. Myers, R.C. Tuckey, A.T. Slominski, D.D. Miller, W. Li, Synthesis and Biological Evaluation of Vitamin D3 Metabolite 20S,23S-Dihydroxyvitamin D3 and Its 23R Epimer, J Med Chem. 59 (2016) 5102–5108. https://doi.org/10.1021/acs.jmedchem.6b00182.

[50] QUATRX PHARMACEUTICALS COMPANY, Efficient process for preparing steroids and vitamin D derivatives with the unnatural configuration at C20 (20 alpha-methyl) from pregnenolone, US 2008/0171728 A1, 2008.

[51] J. Mikus, D. Steverding, A simple colorimetric method to screen drug cytotoxicity against Leishmania using the dye Alamar Blue®, Parasitol Int. 48 (2000) 265–269. https://doi.org/10.1016/S1383-5769(99)00020-3.

[52] T. Sander, J. Freyss, M. von Korff, C. Rufener, DataWarrior: An open-source program for chemistry aware data visualization and analysis, J Chem Inf Model. 55 (2015) 460–473. https://doi.org/10.1021/ci500588j.

[53] D.E.V. Pires, T.L. Blundell, D.B. Ascher, pkCSM: Predicting small-molecule pharmacokinetic and toxicity properties using graph-based signatures, J Med Chem. 58 (2015) 4066–4072. https://doi.org/10.1021/acs.jmedchem.5b00104.